A 3D Printed Hanging Drop Platform for Spheroid Production, Pick-up, and Patterning



Bisan Samara Department of Biomedical Engineering

McGill University, Montreal

December 2023

A thesis submitted to McGill University in partial fulfillment of the requirements of the degree of Master of Engineering

© Bisan Samara, 2023

Table of Contents

Abstract (English)				
Abstract (French)				
Acknowledgement				
Contribution of Authors				
List of Figures				
List of Abbreviations				
1. Chapter 1: Introduction and Literature Review				
	1.1.	Motivation for 3D Cell Culture	8	
	1.2.	Spheroids and Organoids	9	
	1.3.	3D Cell Culture Methods	10	
	1.3.1.	Scaffold-free 3D Cultures	11	
	1.3.1.1.	The Hanging Drop Technique	11	
	1.3.1.2.	Ultra-low Attachment Plates	12	
	1.3.1.3.	Magnetic Levitation	13	
	1.3.2.	Scaffold-based 3D Culture	13	
	1.3.2.1.	Matrix-embedded	14	
	1.3.2.2.	Matrix-encapsulated	14	
	1.3.2.3.	Spinning/rotating Flasks	15	
	1.3.3.	Tissue Explants	15	
	1.3.4.	Microfluidic Devices 3D Cultures	15	
	1.4.	Hanging Drop Platforms in Literature	16	
	1.4.1.	Modified hanging drop plates	16	
	1.4.2.	Hanging drop microfluidic chips	19	
	1.5.	Rationale of This Work	23	
2. Chapter 2: Manuscript				
	2.1.	Abstract	25	
	2.2.	Introduction	26	

	2.3.	Methods	30
	2.3.1.	Cell Culture	30
	2.3.2.	System Manufacturing	30
	2.3.3.	Spheroid Formation	31
	2.3.4.	Spheroid Pick-and-Place	31
	2.3.5.	Cytotoxicity Testing	32
	2.3.6.	Microscopy	33
	2.3.7.	Droplet Characterization	34
	2.3.8.	Data Analysis	34
	2.4.	Results and Discussion	34
	2.4.1.	System Design and Operation	34
	2.4.2.	System Biocompatibility	38
	2.4.3.	Characterization and Cell Culture Optimization	39
	2.4.4.	Patterning and Proof-of-Concept	44
	2.5.	Conclusion	47
	2.6.	Acknowledgements	48
	2.7.	References	48
	2.8.	Supplementary Information	51
3. Chapter 3: Discussion			53
	3.1	Future Perspectives	57
4. Chapter 4: Conclusion			
References			

A 3D Printed Hanging Drop Platform for Spheroid Production, Pick-up, and Patterning

Abstract (English)

Spheroids are 3D cell culture models that offer a higher level of biomimicry compared to 2D culture. Hence, their exploitation in different life-sciences research is rapidly increasing, including but not limited to drug discovery, regenerative medicine, and cancer studies. One of the most common approaches to generate spheroids is the hanging drop technique (HDT), where microliter-sized droplets are suspended for gravity-mediated cell aggregation. Several platforms were engineered to generate spheroids via hanging drops, however, they often have complicated setups, lengthy protocols, difficult manufacturing, and require a lot of manual pipetting steps if robotics is not available. In this work, we developed a modified hanging drop platform to generate spheroids, pick them up once formed, and pattern them on culture surfaces. The entire platform is 3D printed from a biocompatible material that can be put in direct contact with the cells after minimal post-processing steps. Moreover, the process of spheroid formation, pick-up, and transfer is done without the use of pipettes to avoid aggregate disruption and reduce userto-user variability. The platform consists of two main components: aggregation pillars and pickand-place pillars. The former are hollow pillars that are filled with cell suspension via capillary action, then plunger-like structures are inserted into the pillar to push the suspension towards the surface of the pillars where the hanging droplets are stably formed. Once spheroids are generated, the pick-and-place pillars are used to pick-up spheroids and deposit them onto a culture surface according to a pre-determined pattern. Both components are designed to fit within commercial 24-well plates. Our results show that the material used for 3D printing, after minimal post-processing, is cytocompatible for both HT29 colorectal adenocarcinoma and MCF-7 breast cancer cell lines. As a proof of concept for cell aggregation, round, compact spheroids of HT29 and MCF-7 were formed, then picked-and-placed on 24-well plate surfaces. Using 3D printing makes it possible to modulate the design for specific applications. For examples, by changing aggregation pillars diameter, the size of shape of resulting spheroids can be altered. Moreover, by changing the motif of the pick-and-place pillars, different patterns can be generated on well plate surfaces. Patterns of rectangular arrays, circular array, and maple leaf shape were created as a demonstration. The presented platform offers a practical solution to make spheroid production and handling easier. Future directions include testing the platform for the aggregation of other cell types, such as stem cells or primary patient derived cells; as well as further enhancing the design to support more spheroid manipulation steps, such as pipette-less media exchange for prolonged culture.

Abstract (French)

Les sphéroïdes sont des modèles de culture cellulaire 3D qui offrent un niveau plus élevé de biomimétisme en comparaison à la culture 2D. Par conséquent, leur exploitation dans différentes recherches en sciences de la vie augmente rapidement, y compris, mais sans s'y limiter, la découverte de médicaments, la médecine régénérative et les études sur le cancer. L'une des approches les plus courantes pour générer des sphéroïdes est la technique de la goutte suspendue, où des gouttelettes de la taille d'un microlitre sont suspendues pour l'agrégation cellulaire médiée par gravité. Plusieurs plates-formes ont été conçues pour générer des sphéroïdes via des gouttes suspendues, cependant, elles ont souvent des configurations

compliquées, des protocoles longs, une fabrication difficile et nécessitent beaucoup d'étapes de pipetage manuelles si la robotique n'est pas disponible. Dans ce travail, nous avons développé une plate-forme de chute suspendue modifiée pour générer des sphéroïdes, les ramasser une fois formés et les modeler sur des surfaces de culture. L'ensemble de la plate-forme est imprimé en 3D à partir d'un matériau biocompatible qui peut être mis en contact direct avec les cellules après des étapes minimales de post-traitement. De plus, le processus de formation, de ramassage et de transfert de sphéroïdes se fait sans l'utilisation de pipettes pour éviter les perturbations globales et réduire la variabilité d'utilisateur à utilisateur. La plate-forme se compose de deux composants principaux: les piliers d'agrégation et les piliers ramasser-et-placer. Les premiers sont des piliers creux qui sont remplis de suspension cellulaire par action capillaire, puis des structures en forme de piston sont insérées dans le pilier pour pousser la suspension vers la surface des piliers où les gouttelettes suspendues sont formées de manière stable. Une fois les sphéroïdes générés, les piliers ramasser-et-placer sont utilisés pour ramasser les sphéroïdes et les déposer sur une surface de culture selon un modèle prédéterminé. Les deux composants sont conçus pour s'adapter à des plaques commerciales de 24 puits. Nos résultats démontrent que le matériel utilisé pour l'impression 3D, après post-traitement minimal, est cytocompatible pour l'adénocarcinome colorectal HT29 et les variétés de cellule MCF-7 de cancer du sein. Comme preuve de concept pour l'agrégation cellulaire, des sphéroïdes ronds et compacts de HT29 et MCF-7 ont été formés, puis cueillis et placés sur des surfaces de plaques de 24 puits. L'utilisation de l'impression 3D permet de moduler la conception pour des applications spécifiques. Par exemple, en modifiant le diamètre des piliers d'agrégation, la taille de la forme des sphéroïdes résultants peut être modifiée. De plus, en modifiant le motif des piliers ramasser-et-placer,

différents motifs peuvent être générés sur les surfaces des plaques de puits. Des motifs de tableaux rectangulaires, de cercles cocentriques et de forme de feuille d'érable ont été créés à titre de démonstration. La plate-forme présentée offre une solution pratique pour faciliter la production et la manipulation des sphéroïdes. Les orientations futures comprennent la mise à l'essai de la plateforme pour l'agrégation de d'autres types de cellules, comme les cellules souches ou les cellules dérivées de patients primaires; ainsi que l'amélioration de la conception pour prendre en charge plus d'étapes de manipulation des sphéroïdes, telles que l'échange de médias sans pipette pour une culture prolongée.

Acknowledgement

I would like to express my heartfelt gratitude to all those who have supported and contributed to the successful completion of this master's thesis.

First and foremost, I am grateful to my thesis advisor, Dr. David Juncker, for his invaluable support throughout this research journey. His mentorship and dedication have been instrumental in shaping the direction of this work and have inspired me to strive for excellence. I would also like to thank all the professors and colleagues who I worked with during my undergraduate and post-graduate research experiences prior starting my master's at McGill. I am grateful for everything I learned from you.

A special thank you to everyone at the Juncker Lab for generously sharing their knowledge and expertise, and providing a nurturing, supportive academic environment that allowed me to delve into my research with passion and curiosity.

This thesis would not have been possible without the endless love and support of my parents Hend and Salim. I am deeply grateful for the sacrifices you both made, ensuring that I had access to the best education and opportunities. Words cannot express how indebted I am for all you have done, and still do. A big thank you for my loving siblings: Haneen, Salam, and Abood, my brother-in-law Mohammad, and my joyful niece and nephew, Leen and Karam. Thank you for being my pillars of support, for cheering me on every triumph and offering words of comfort during moments of challenge. I am forever grateful for everything you have done for me.

A special thank you to my husband, Ahmed, who I was extremely lucky to meet during my studies at McGill. I am glad to have spent the second half of my program by your side. Thank you for your love, support, and patience during this time. You definitely made the journey more fun to go through! Your belief in my abilities, even during moments of self-doubt, has been a constant source of strength and motivation.

Lastly, I would like to thank the Biomedical Engineering Department at McGill for generously supporting my master's with a recruitment award and an excellence award. I am also thankful for the Natural Sciences and Engineering Research Council of Canada (NSERC) for contributing towards funding my master's degree.

Contribution of Authors

The thesis and manuscript were written by Bisan Samara, with feedback from Dr. David Juncker. Dr. Ahmed Abou-Sharkh translated the abstract from English to French. The idea of the project was formulated by Bisan Samara and David Juncker. All experiments were carried out by Bisan Samara, with guidance and support from Dr. David Juncker. The design of the 24-well compatible

base of the aggregation and pick-up pillars was adapted from previous work by Grant Ongo. The patterning protocol was also adapted from Grant Ongo's work with modifications. The formula of the resin used for 3D printing was optimized by Dr. Vahid Karamzadeh. The cells used in this work were transfected with GFP or TdTomato by Molly Shen. Professional images for the setup in manuscript figure 2 were taken by Yonatan Morocz.

List of Figures

Chapter 1

- Figure 1. Comparing organoids and spheroids
- Figure 2. Schematics illustrating different 3D culture methods
- Figure 3. Summary of Hanging Drop Plates in Literature
- Figure 4. Summary of Hanging Drop Microfluidic Chips in Literature

Chapter 2

- Figure 1. Simplified schematics of the workflow of the system
- Figure 2. The system and the workflow
- Figure 3. Cytotoxicity test of PEGDA
- Figure 4. Effect of media additives on aggregating HT29 and MCF-7 cells
- Figure 5. Effect of changing aggregation pillar diameters on HT29 and MCF-7 spheroids
- Figure 6. Optimizing hollow channel diameter in aggregation pillars

Figure 7. Patterning and Proof-of-Concept

Supplementary Figure 1. SolidWorks drawings annotated with dimensions of the system **Supplementary Figure 2.** Top view for SolidWorks drawings of pick-and-place pillars used to create all patterns

List of Abbreviations

HDT Hanging drop technique

ECM Extracellular matrix

ULA Ultra-low attachment

PMMA Poly(methyl methacrylate)

PBS Phosphate buffered saline

PET Polyethylene terephthalate

PEGDA Poly(ethylene glycol) diacrylate

PABO Phenylbis(2,4,6-trimethylbenzoyl)phosphine oxide

ITX Isopropylthioxanthone

MethoCel Methylcellulose

OD Optical density

POMaC Poly(octamethylene maleate (anhydride) citrate)

PDL Poly-D-lysine

1. Chapter 1: Introduction and Literature Review

1.1. Motivation for 3D Cell Culture

Three-dimensional cell culture models are becoming increasingly popular in biological research. Unlike growing cell on flat, two-dimensional surfaces, 3D cell culture models allow cells to grow in a more natural environment that better mimics cell-cell and cell-extracellular matrix (ECM) interactions in vivo. On average, it takes a drug twelve years to progress from bench to market, and costs over two-billion dollars; with a quarter typically going for efficacy screening assays and toxicity testing^{1,2}. Strikingly, more than 90% of drugs that pass pre-clinical stages fail during clinical trials, wasting huge investments and efforts for pharmaceutical companies^{1,2}. Part of this failure is attributed to the discrepancies between the pre-clinical testing environments and the human body environment³. Most in vitro drug efficacy and toxicity testing rely on simplistic twodimensional colorimetric assays that are far from representing the complexity of human tissues and organs. Moreover, although animal models are important to understand certain biological phenomena, the anatomy and physiology of animals is profoundly different from that of the human⁴, and there are ethical concerns regarding the use of animals in scientific research. These challenges resulted in a "productivity crisis" in the pharmaceutical industry, making it unable to meet the needs of the ageing population and limited healthcare budgets⁵. 3D cultures offer a more physiologically relevant cell morphology, polarity, nutrient uptake, growth kinetics, signalling pathways, as well as protein and gene expression profiles⁶; Making them invaluable tools for in vitro drug screening studies, and eliminating the need for animal testing in some cases⁶.

On another note, 3D cultures proved superior in treating several conditions through regenerative medicine, such as wound healing⁷, heart failure⁸, and liver damage⁹. They have been used in *in vitro* studies of cell/tissue behaviour and disease mechanisms. Furthermore, when 3D cultures are made from patient-derived cells, they can be used to personalize treatment plans *in vitro*, before administering them on the patient.

1.2. Spheroids and Organoids

Driven by these numerous advantages, the number of scientific publications with the key words "organoid" and "spheroid", the most commonly used 3D culture, witnessed an exponential increase within the past two decades (Figure 1A). This was accompanied by the establishment of several companies that focus on producing 3D cultures for drug screening and other applications, such as InSphero Inc. (Schlieren, Switzerland), HUB Organoids (Utrecht, Nederland), Cellesce Ltd (Cardiff, UK), and many others.

Spheroids are 3D cell aggregates brought together by cell-cell adhesion resulting from the upregulation of E-cadherin^{4,10}. They are typically made of cell lines, but can also be made of primary cells^{4,10}. On the other hand, organoids are 3D multicellular structures derived from stem cells that are capable of self-renewal and self-organization with spatially constrained lineage commitment^{4,10}. Despite the high level of complexity and biomimicry of organoids, their utilization is hindered by the relatively high cost of production, lack of protocol standardization, and challenges in obtaining high-fidelity cells^{4,11,12}. Spheroids do not require an ECM or growth factors¹⁰, which makes them easier and less expensive to culture. Figure 1B provides a summary of the key differences between spheroids and organoids.

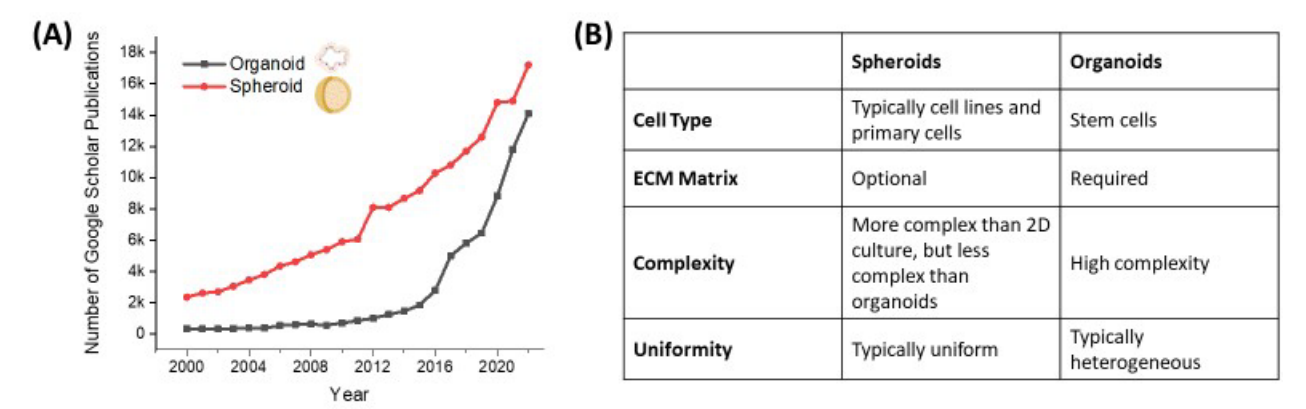


Figure 1. Comparing organoids and spheroids. (A) number of publications in google scholar search for the key words "organoid" and "spheroid" between 2000 and 2022. (B) comparison table summarizing key differences between organoids and spheroids based in information reported in literature $^{4,10-12}$.

1.3. 3D Cell Culture Methods

Several methods have been reported to make 3D cultures. This includes culturing cells as scaffold-free constructs, tissue explants, scaffold-embedded constructs, and microfluidic devices^{6,13–15}. Each method offers some advantages as well as limitations and challenges, making some methods more suitable for certain applications than others. The following sections will elaborate on each method of 3D cultures. All methods are summarized in 2.

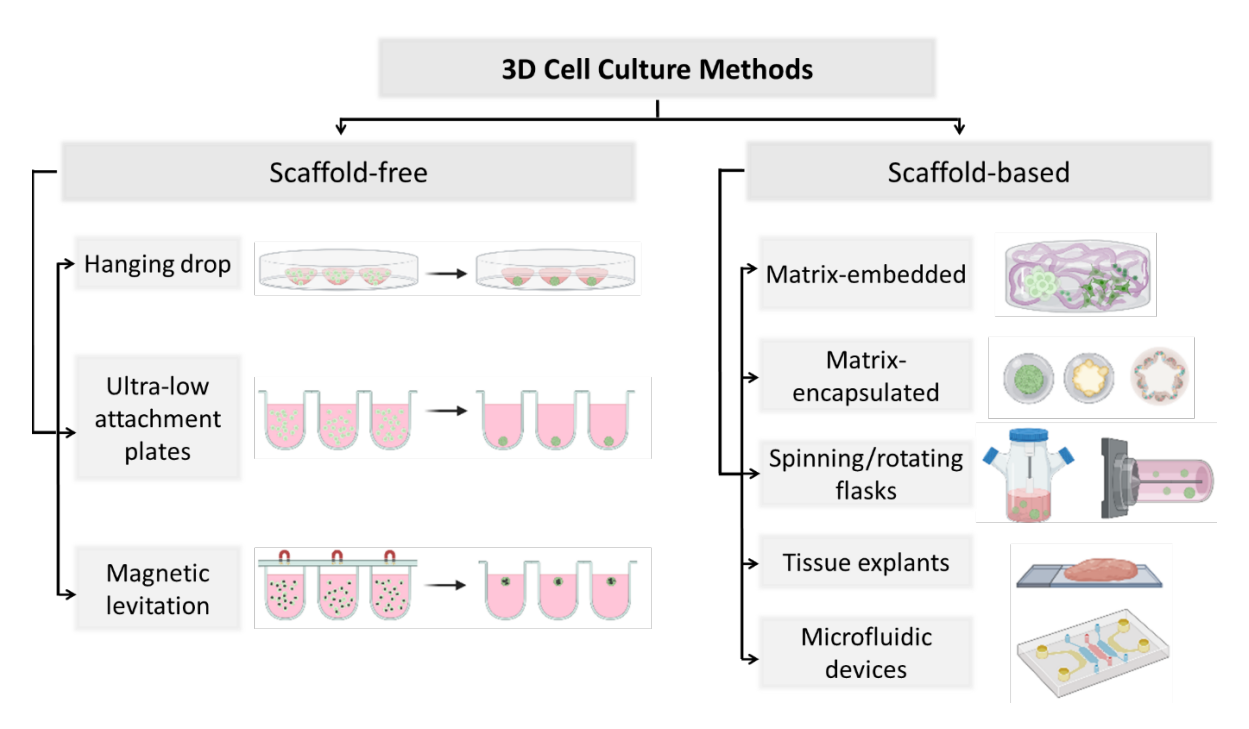


Figure 2. Schematics illustrating different 3D culture methods as classified in section 1.3. Figure created with BioRender.com.

1.3.1. Scaffold-free 3D Cultures

Scaffold-free cultures rely on the aggregation of cells into highly organized, non-adherent 3D constructs. There are several ways to facilitate cell aggregation in a scaffold-free manner, including the HDT, ultra-low attachment (ULA) plates, and magnetic levitation.

1.3.1.1. The Hanging Drop Technique

In the HDT, microliter-sized cell suspensions (< $50 \, \mu$ L) are pipetted on the inner surface of the lid of a petri dish and flipped for gravity mediated sedimentation of cells at the at the liquid-air interface. The lid is then placed on a petri dish filled with sterile liquid, typically phosphate buffered saline (PBS) or distilled water, to prevent droplet evaporation. After 1-3 days of incubation, spheroids or organoids are formed^{4,13–15}. The size of the formed constructs can be

controlled by the initial cell concentration in the droplet¹⁵, and the shape is largely determined by the curvature of the hanging droplet¹⁶.

The HDT is considered the most advanced method for spheroid production¹⁵. While it is a relatively inexpensive approach to produce 3D cultures, it has some limitations. The HDT suffers from highly manual protocols if robotics is not available, and susceptibility of droplet detachment due to dish titling, flipping, or shaking during culture. It requires technical expertise and can be time-consuming, specially when a large number of constructs are needed. Section 1.4 reviews several tools that were developed to overcome the challenges faced with the conventional HDT.

1.3.1.2. Ultra-low Attachment Plates

ULA plates are cell culture plates coated with an inert, non-adherent polymers, such as agarose or poly(2-hydroxyethyl methacrylate)^{13,15}. This way, the cells will favor the formation of cell-cell bonds rather than cell-substrate bond. Some ULA plates have round or conical bottoms to further help with the aggregation and positioning of the forming 3D construct.

Unlike HDT, aggregation with ULA plates allow for using bigger amounts of culture medium without compromising the stability of the aggregate. Moreover, the aggregates in this method are less sensitive to plate tiling or movement. In addition, since ULA plates typically come in a standard well-plate format (384- or 96-well), this method is more compatible with the use of robotics for high-throughput generation of 3D constructs. However, if robotics are not accessible, the process is highly manual and susceptible to user-to-user variability in same way it is for the HDT. Whether to use hanging drops or ULA plates depends on the tools and facilities available. It also depends on the cell type used. Some cells, such as human ovarian carcinoma (OVCAR8) and

human breast cancer (MCF-7) cell lines, form more compact aggregates with the HDT^{17,18}. While other cells, such as primary osteoblasts and endothelial cells, aggregate better in ULA plates¹⁹.

1.3.1.3. Magnetic Levitation

In magnetic levitation culture, magnetic nanoparticles are internalized by cells and placed in a magnetic field to overcome gravitational forces, causing them to elevate and aggregate. This method allows for a quick aggregation in less than a day, however, nanoparticles can be toxic and costly, some cells do not digest them properly, and they may interfere with certain experimental techniques, such as microscopy or magnetic resonance imaging (MRI)^{4,13,14}.

1.3.2. Scaffold-based 3D Culture

In scaffold-based 3D culture, cells are grown in a 3D scaffold. The physical (e.g. porosity), mechanical (e.g. stiffness), or chemical and biological (e.g. nutrient gradients, growth factors, ligands, etc.) properties of the scaffold can be modified to promote certain cell phenotype or activity^{15,20}. Scaffolds used in this method can be of natural sources, synthetic, or a mixture of both. Natural scaffolds, such as collagen, Matrigel, or fibrin, are widely used in 3D cell culture due to their biocompatibility and favourable adhesive properties that promote cell growth and functions. It s possible to tune the porosity, pore size, and stiffness of some hydrogels by changing the concentration and/or gelation temperatures¹⁵. A main limitation of natural scaffolds is the batch-to-batch variability, which is overcome by synthetic scaffolds that have well-defined properties designed for specific applications. Thus, synthetic scaffolds are more reproducible and their properties are easier to tune for desired outcomes^{14,15}. Examples of common synthetic scaffolds include Polyethylene glycol (PEG) and polylactic acid (PA). These scaffold usually need

to be functionalized with biological peptides for improved cell adhesion and proliferation¹⁵. Scaffold-based techniques can be classified into matrix-embedded, matrix-encapsulated, and spinning/rotating flasks.

1.3.2.1. Matrix-embedded

In this technique, cells are suspended in the liquid precursor of a hydrogel in a well. As the hydrogel crosslinks, the cells will be embedded within the 3D architecture of the matrix allowing for cell-cell and cell-matrix interactions. Whether the cells are embedded as single cells or aggregated depends on the cell type and its potential to aggregate, and the presence of agitation forces during gelation¹⁴. On another note, it is controversial when cells are seeded on top of 3D matrices rather than within them. Some studies consider this configuration as 3D culture, while others refer to this configuration as 2.5D culture. A. Zerda el al. defined 2.5D culture as cells grown on non-flat substrates with topological features that interact with the basal membranes cultured on top of them, while the apical surface is still free²¹.

1.3.2.2. Matrix-encapsulated

Here droplets of cells suspensions are entrapped within a hydrogel shell that is chemically crosslinked afterwards. Matrix-encapsulation is typically done using microfluidic devices for droplets generation and entrapment^{14,20}. It could also be done by manually sandwiching the 3D construct in hydrogel droplets via a pipette. Matrix-encapsulation is mostly used for organoid culture.

1.3.2.3. Spinning/rotating Flasks

In the spinning flask method, cells are cultured within stationary scaffolds placed inside a flask filled with medium under continuous agitation, typically via a magnetic stirring bar. Rotating flasks work in a similar manner, except that here the flask itself rotates continuously, exerting less shear forces on the cells. The continues agitation in both methods ensures good distribution of oxygen and nutrients throughout the medium, and the spinning/rotation speed can be adjusted to control the sizes of the forming 3D constructs. Although these methods are good to generate large amounts of 3D constructs, they often result in constructs of heterogeneous shapes. Moreover, the continuous agitation makes it hard to visualize the aggregates or image them^{4,13,14}.

1.3.3. Tissue Explants

This is one of the earliest attempts of culturing 3D constructs. In this method, 3D tumor tissue is extracted from the patient, cleared of any necrotic parts, and cultured on collagen coated flask. A key advantage of this approach is the preservation of the natural tumor microenvironment in terms of cell components as well as ECM. However, the limitations include high heterogeneity resulting in poor reproducibility of results, and difficulties in obtaining tissue donors¹⁴.

1.3.4. Microfluidic Devices 3D Cultures

The term microfluidics refers to the field of manipulating fluids and particles, with high precision and accuracy, in devices with micrometer scale structures. Examples of such structures include microchannels, reservoirs, microvalves, and micropumps^{22,23}. Microfluidic devices were originally used in the semiconductors industry²⁴, but got quickly adopted in other fields including life-

sciences and tissue engineering due to their numerous advantages. Microfluidic devices enable studying small amounts of samples and reagents relatively quickly, and at low cost. Moreover, for cell culture applications, such devices are typically made of poly(dimethylsiloxane) (PDMS) which is a biocompatible, optically transparent, and oxygen-permeable polymer^{13,22}. Moreover, microfluidic devices allow introducing flow to the culture system, mimicking physiological shear stresses and nutrient exchange. They also enable the compartmentalization of cell residents making it possible to develop co-culture models to study complex interactions across tissues.

Driven by advances in microfluidics and tissue engineering, the field of organ-on-a-chips emerged to focus on recreating precise aspects of the cellular, geometrical, chemical, and mechanical microenvironment of human tissues and organs.

1.4. Hanging Drop Platforms in Literature

Several research groups engineered hanging drop platforms that overcome one or more limitation of the conventional HDT. In this section, these platforms will be grouped into two categories: hanging drop plates and hanging drop microfluidic chips. The former are platforms that are essentially in the format of a modified well-plates. While the latter category refers to devices that do not necessarily have the format of a well plate. These devices utilize one or more microfluidic flow phenomena such as capillary flow or surface tension in the formation or transfer of droplets, and some are connected to external instruments such as fluidic pumps.

1.4.1. Modified hanging drop plates

One of the most notable hanging drop plates was developed by the research group of professor Shuichi Takayama²⁵. The plate is fabricated from polystyrene by injection molding. It has the

format of a 384-well plate, with hollow conduits of 1.6 mm diameter at the center of each well site (Figure 3A)²⁵. The bottom side of the conduit has a plateau of 3 mm diameter that defines the borders of the hanging drop. For cell seeding, a pipette tip is inserted through each conduit from the top side, ten to twenty microliters of cell suspension solution is pipetted, and the pipette tip is removed leaving the hanging droplet behind²⁵. For humification, the periphery of the plate has a built-in water reservoir, and the plate was mounted on a 96-well plate filled with distilled water and the entire setup was wrapped with parafilm. The open top side is also used for medium exchange and spheroid retrieval using a regular pipette or liquid handling robots²⁵.

Another platform, developed by B. Gao et al. ¹⁶, used laser etching to make concentric rims on poly(methyl methacrylate) (PMMA) (Figure 3B). The rims help to control the spreading of the hanging droplet due to liquid pinning. The PMMA piece has 24 etched units following a standard 24-well plate format. Around each main unit, four concentric circles were etched to serve as a backup in case the droplet crossed the smaller rims. In this platform, the geometry of the hanging drop is determined by the surface tension that is proportional to the spreading rim, and the gravitational force governed by the volume of the droplet ¹⁶. For cell seeding, cell suspension is manually pipetted on the surface of the PMMA plate, the plate is then flipped and mounted on

top of a 24-well plate filled with Phosphate buffered saline (PBS) for humidification. Retrieval of the spheroids is done manually with a pipette if needed.

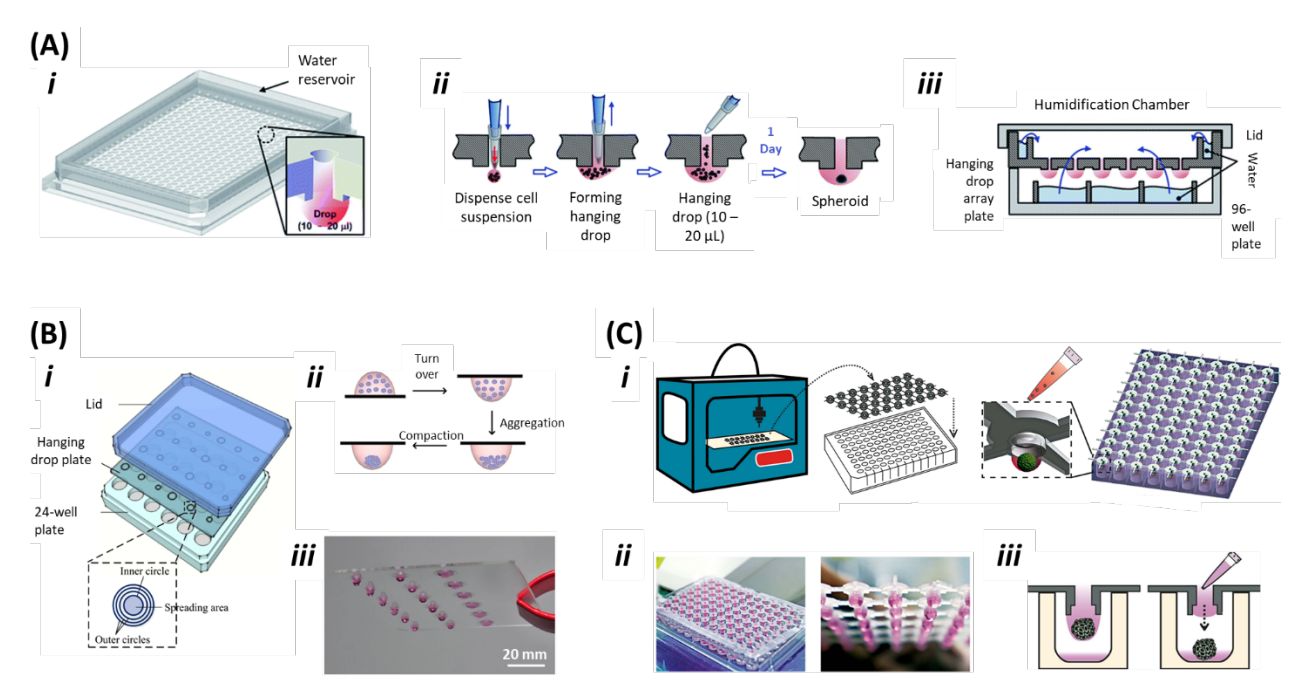


Figure 3. Summary of Hanging Drop Plates in Literature. (A) i. Schematics of the hanging drop plate developed by Y. Tung et al.²⁵. ii. The process of cell seeding and spheroid formation explained in a close-up schematic of one well. iii. Schematics of the setup used for humification and incubation. (B) i. Schematics of the hanging drop plates developed by B. Gao et al.¹⁶. ii. Schematics of the cell seeding and spheroid formation process. iii. An image of a PMMA device loaded with hanging droplets of varying rim diameters to control the spreading area of the droplet. (C) i. Schematics of the 3D printed mesh insert used for aggregation and developed by L. Zhao et al.²⁶. ii. Images of the mesh mounted on a 96-well plate (left) and a close-up image of the mesh with hanging drops (right). iii. Schematics of the dripping step explained on one well. All images were adapted with permission from their respective publisher.

A more recent study by L. Zhao et al.²⁶ utilized 3D printing to fabricate a mesh-like insert with through-holes that correspond to 24-, 96- or 384-well plates (Figure 3C). For cell seeding, the 3D printed insert is mounted on top of the well plate of choice, cell suspension in manually pipetted

in each through-hole, and the plate Is covered with its lid. For humification, culture medium is added to the wells. After aggregation, spheroid retrieval is done by either by adding drops of liquid on top of the through-hole with the hanging droplet until it drips into the well, or by allowing the hanging droplet to drip spontaneously. Hence, the authors called this platform the "3D Printed Hanging Drop Dripper"²⁶. The configuration of this plate allows studying metastasis by dripping the spheroids onto a well with an ECM gel, interaction between two cell types by dripping the spheroid onto a well with a monolayer of a different cell type (e.g. tumor spheroid and endothelial cell monolayer), or interaction between two spheroids by modulating the insert to have two adjacent through-holes for two spheroids that drip into the same well²⁶.

1.4.2. Hanging drop microfluidic chips

As mentioned in section 1.3.4 previously, microfluidics technology offers numerous advantages when it comes to controlling minute amounts of liquids. Several studies utilized this technology to overcome some limitations of the conventional HDT. For example, O. Frey et al. developed a PDMS-based microfluidic device with serially connected open circular grooves, surrounded by hydrophobic rims to limit droplet spreading (Figure 4A)²⁷. The device is fabricated by photolithography from a two-layer SU-8 mold. After PDMS is casted and cured, the devices are peeled-off, inlet/outlet holes are punched, and each device is bonded to a glass slide with drilled holes. Cell seeding to all open rings is done by perfusing the inlet with cell suspension either with a standard pipette or with a syringe pump, the suspension fills the conduits via capillary forces, and with the increasing pressure, droplets start forming beneath the circular grooves. Eventually, pressure equilibrium due to the surface tension at the liquid–air interface, all interconnected droplets will have the same size and volume²⁷. Once the cells aggregate, the formed tissues can

be harvested by aspirating a few microliters from the bottom of the droplet, or by contacting the chip with a flat plate. A key advantage of this system is that it makes it possible to create complex microfluidic networks of various configurations by introducing flow control elements, such as micro-valves and gradient generators. As a result, the system can be used to aggregate different cell types in adjacent, but not interconnected, openings. Moreover, different culture conditions (e.g. drug concentrations or flow) can be applied aggregates in selected wells²⁷.

T. E. de Groot et al. developed a suspended microfluidic hanging drop chip made of CNC milled polystyrene with two through-holes, one slightly larger than the other, connected with an open top channel (Figure 4B)²⁸. The basic concept is using on of the through-holes to form a cell aggregating hanging droplet, and the other one as a suspended cell-free reservoir for medium exchange. For cell seeding, each device is filled with sixty microliters of culture medium, then two microliters of cell suspension is added to the larger through-hole, referred to as the culture well, and allowed to aggregate for at least a day. The difference in well diameters result in a pressure difference that shifts the flow direction towards the cell-free well when fluid is aspirated, and visa versa when fluid is added (Figure 4B). This way, it is possible to perform medium exchange without performing any fluid operations directly on the culture well, and therefore, protecting the aggregating from potential disruptions resulting from repeated pipetting steps²⁸.

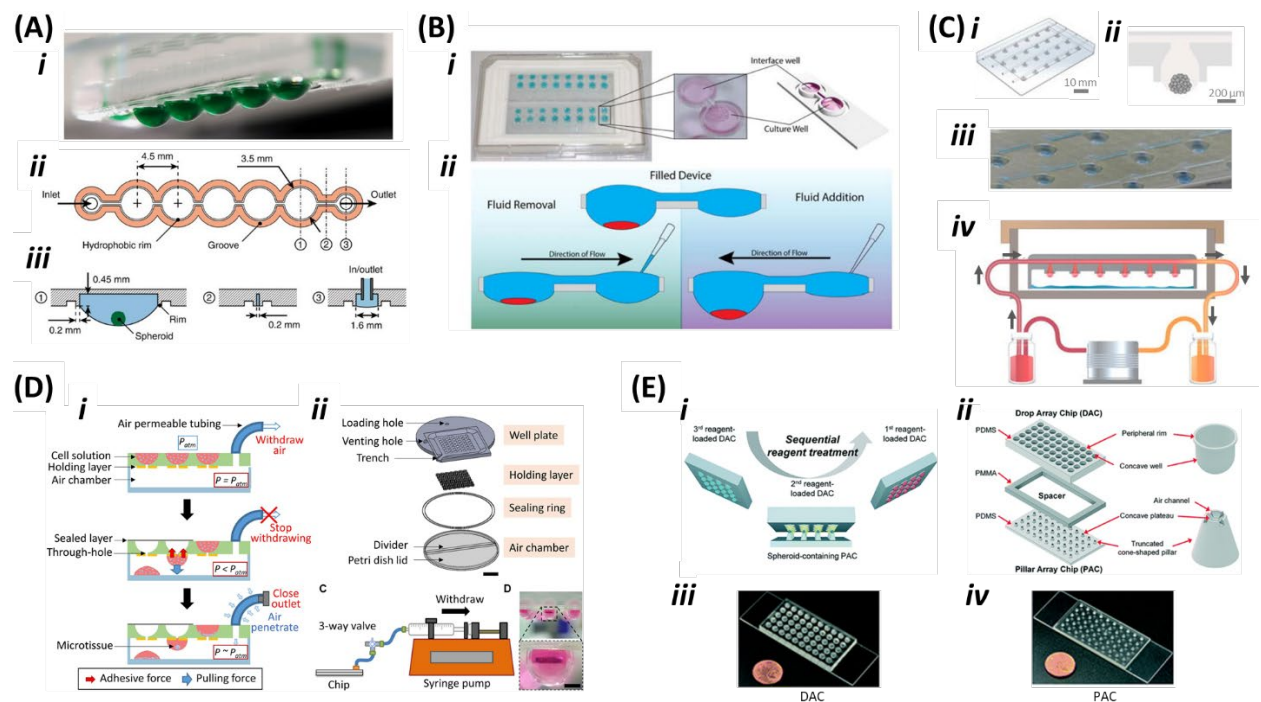


Figure 4. Summary of Hanging Drop Microfluidic Chips in Literature. (A) i. Image of the microfluidic devices developed by O. Frey et al.²⁷ filled with colored water. ii. Annotated drawing for the design of the device. iii. Cross-sectional drawings as shown in Aii. (B) i. Image of the suspended microfluidic platform developed by T. E. de Groot et al.²⁸ with a zoomed-in schematic for a single device. ii. Schematics of a filled device explaining how the flow shifts when fluid is added or removed from the cell-free well. (C) i. Schematics of the hanging drop microfluidic chip developed by S. Huang et al.²⁹. ii. Close-up illustration on one well. iii. Image of a device filled with colored water. iv. Schematics showing the device with the humification chamber, with the inlet/outlet connected to a peristaltic pump. (D) i. Schematics illustrating the working principle of the pressure assisted platform engineered by C. Cho et al. 30. ii. Exploded view of the main components of the platform (Scale bar is 2 cm). iii. Schematics showing the setup with the chip connected to a syringe pump to create negative pressure. (E) i. Schematics of the hanging drop platform developed by H. Kim et al.31, showing a PAC containing spheroids, and multiple DACs loaded with different reagents to be sequentially delivered to the spheroids. ii. Exploded view of the main components of the platform, with close-ups on a well of the DAC and pillar of the PAC. iii. and iv. Images of the DAC and PAC, respectively, bonded on a glass slide. All images were adapted with permission from their respective publisher.

S. Huang et al.²⁹ developed a microfluidic system, made of PMMA, with 4 x 6 open, conical wells for the formation and perfusion of hanging drops (Figure 4C). The system consists of three layers: a top layer with four sets of inlets and outlets, a middle layer with four channels for liquid flow, and a bottom layer with six open wells, or through-holes, for cell aggregation via the HDT. The first two layers are fabricated by laser ablation, while the bottom layer is fabricated by three-axis CNC grinding. Each of the four channels in the middle layer supplies medium for a line of six hanging drop wells. For cell seeding, the channels are first filled with medium via a peristaltic pump, cell suspension is pipetted into each well, chip is flipped upside down, and the hanging droplets increase in size with liquid pressure. An optimized flow rate was applied at the inlets and outlets, and flow is continuous for medium replenishment.

Another study published around the same time reports a "pressure-assisted network for droplet accumulation"³⁰. The basic principle of the system (Figure 4D) relies on the pressure difference between the external environment and the internal chamber for hanging drop formation. The system comprises four main parts: well plate, holding layer, sealing ring, and an internal air chamber. The well plate, made of a CNC machined polycarbonate sheet, has well shaped as half spheres, with an open slit at the center where the hanging drops will form. The holding layer, made of hydrophilic polyethylene terephthalate (PET), has connecting rings that are complementary in geometry to the bottom of the well of the well plate. The purpose of this layer is to prevent droplet spreading. The air chamber is essentially a standard 90 mm petri dish lid with a CNC machined divider that creates two reservoirs; one for humidification of the droplet, and the other will be connected later to a suction syringe pump to create negative air pressure. Finally, the sealing ring, made of PET, is used to ensure tight fit during air withdrawal. For cell

seeding, one pipetting step is needed on top of the well plate, excess suspension is removed through a side trench, half of the petri dish lid is filled with PBS then the opening is sealed with tape, the syringe pump is connected via tubing and suction is started until all the droplet are formed, then the wells are sealed the droplets are left to aggregate in the incubator. Formed spheroids are collected individually with a pipette from the bottom side of the well plate after the system is disassembled³⁰.

More recently, H. Kim et al. developed a system for the formation and contact-based transfer of spheroids³¹. The system consists of two main parts: a drop array chip (DAC) and a pillar array chip (PAC) (Figure 4E). Both parts are made of PDMS replicas from 3D printed molds, and then attached bonded to glass slides. The DAC has an array of concave wells, of 3 mm diameter and height, onto which cell suspension or reagents are pipetted then flipped to form hanging drops or load reagents for fluid exchange, respectively. The PAC has a matching array of truncated, conical pillars with concave apical surfaces for the pick-up and transfer of spheroids from the DAC. The surface of the PAC also has air vents to ensure spheroid pick-up and positioning at the center of each pillar. During the spheroid transfer process, a spacer is placed between the DAC and PAC for consistent spacing. After spheroid pick-up, more liquid handling processes can be carried out using other sets of DACs, loaded with the needed reagents (e.g. fresh medium), and repeating the same steps³¹.

1.5. Rationale of This Work

Several platforms were engineered to improve the conventional HDT, however, some limitations persist. Majority of the platforms mentioned above still require a pipetting step into each

"hanging drop well" for initial cell seeding, which is laborious if robotics is not accessible or compatible with the platform. Moreover, some platforms jeopardize the practicality of the design when developing devices based on complex microfluidic concepts that require highly skilled personnel to operate and peripheral equipment attached to the system, such as fluid pumps. Not to mention the fine tuning required for key parameters, such as pressure, flow rates, and surface characteristics. Furthermore, the manufacturing process of the platforms often involves multiple molding steps, or specialized instruments. This work aims to provide an improved hanging drop platform that offers simplicity of manufacturing as well as operation, incorporating useful design features from existing platforms, and further improving them certain aspects to make it more user-friendly. The provided solution is 3D printed from a biocompatible material that can be used for cell culture, which decreases post-processing procedures, eliminates the need for moulding steps, and offers higher degrees of design freedom in a cost-effective manner. Moreover, the platform does not require to be attached to bulky specialized equipment, making it more accessible to different labs, and reducing the lab space required to use it.

2. Chapter 2: Manuscript

A 3D Printed Hanging Drop Platform for Spheroid Production & Pick-and-Place

Bisan Samara¹, Grant Ongo¹, Vahid Karamzadeh¹, David Juncker^{1,2‡}

¹Biomedical Engineering Department, McGill University, Montreal, QC, Canada ²McGill Genome Centre, McGill University, Montreal, QC, Canada [‡]Corresponding author

2.1. Abstract

Spheroids are biomimetic 3D cultures that offer a higher complexity compared to 2D cultures. One of the most common approaches to generate spheroids is the hanging drop technique (HDT), where microliter-sized droplets are suspended for gravity-mediated cell aggregation. Several platforms were engineered to generate spheroids via hanging drops, however, they often have complicated setups, lengthy protocols, difficult manufacturing, and require a lot of manual pipetting steps if robotics is not available. In this work, we developed a 3D printed modified hanging drop platform to generate spheroids, pick them up once formed, and pattern them on culture surfaces. The platform consists of two main components: aggregation pillars and pickand-place pillars. The former are hollow pillars that are filled with cell suspension via capillary action, then plunger-like structures are inserted into the pillar to push the suspension towards the surface of the pillars where the hanging droplets are stably formed. Once spheroids are generated, the pick-and-place pillars are used to pick-up spheroids and deposit them onto a culture surface according to a pre-determined pattern. Our results show that the material used for 3D printing, after minimal post-processing, is cyto-compatible for both HT29 colorectal adenocarcinoma and MCF-7 breast cancer cell lines. As a proof of concept for cell aggregation,

round, compact spheroids of HT29 and MCF-7 were formed. Moreover, circular arrays of HT29 cells were generated with 72% success rate. To demonstrate the potential of the platform, patterns of rectangular arrays, circular arrays, and maple leaf shape were created. The presented platform offers a practical solution to make spheroid production and handling easier. Future directions include testing the platform for the aggregation of other cell types, such as stem cells or primary patient derived cells; as well as further enhance spheroid pick-and-place to increase patterning transfer rate.

2.2. Introduction

The past two decades witnessed a significant increase in the use of 3D culture models since they better mimic *in vivo* cell-cell and cell-extracellular matrix (ECM) interactions. This is particularly advantageous in the drug development process, where the discrepancies between the preclinical testing and native tissue environments contribute to a high failure rate of more than 90% of drugs, causing massive financial losses pharma for companies and delaying the progress of novel medications to patients who need it the most^{1–3}. Most *in vitro* drug efficacy and toxicity testing are based on reductionist two-dimensional colorimetric assays that fail to represent the intricacy of human tissues and organs. Moreover, the use of animal models is surrounded by ethical concerns, not to mention that the anatomy and physiology of animals are profoundly different from that of the human⁴. 3D cultures offer a more physiologically relevant cell morphology, polarity, nutrient uptake, growth kinetics, signalling pathways, as well as protein and gene expression profiles⁵; Making them invaluable tools for *in vitro* drug screening studies, and eliminating the need for animal testing in some cases⁵. 3D cultures also proved effective in

various regenerative medicine applications such as helping with the treatment of wound healing⁶, heart failure⁷, and liver damage⁸.

Spheroids are among the most popular 3D culture models. They are 3D cell aggregates brought together by cell-cell adhesion resulting from the upregulation of E-cadherin^{4,9}. Spheroids are typically made from cell lines, and occasionally from primary cells^{4,9}. Unlike organoids, spheroids lack the capability of self-renewal and self-organization. Moreover, they do not require an ECM or growth factors⁹, which makes them easier and less costly to culture.

Several methods have been reported to make spheroids. The hanging drop technique (HDT) is among the most advanced ones¹⁰. Traditionally, in the HDT, microliter-sized cell suspensions (< 50 µL) are pipetted on the inner surface of the lid of a petri dish and flipped for gravity mediated sedimentation of cells at the at the liquid-air interface. The lid is then placed on a petri dish filled with sterile liquid, typically phosphate buffered saline (PBS) or distilled water, to prevent droplet evaporation. After 1-3 days of incubation, spheroids or organoids are formed^{4,10–12}. The size of the formed constructs can be controlled by the initial cell concentration in the droplet¹⁰, and the shape is mainly determined by the curvature of the hanging droplet¹³. While it is a relatively inexpensive approach to produce spheroids, it has some limitations. The HDT suffers from highly manual protocols if robotics is not available, and susceptibility of droplet detachment due to dish titling, flipping, or shaking during culture. It requires technical expertise and can be time-consuming, specially when a large number of constructs are needed.

Several research groups developed hanging drop platforms that overcome one or more limitation of the conventional HDT. For example, Y. Tung et al.¹⁴ engineered a polystyrene 384-well plate

with hollow conduits at the center of each well site where cells are aggregated. The plate is fabricated via injection molding. For cell seeding, a pipette tip is inserted through each conduit from the top side, ten to twenty microliters of cell suspension solution is pipetted, and the pipette tip is removed leaving the hanging droplet behind¹⁴. Moreover, O. Frey et al.¹⁵ developed a PDMS-based hanging drop microfluidic device with serially connected open circular grooves, surrounded by hydrophobic rims to limit droplet spreading¹⁵. The device is fabricated by photolithography from a two-layer SU-8 mold. After PDMS is casted and cured, the devices are peeled-off, inlet/outlet holes are punched, and each device is bonded to a glass slide with drilled holes. Cell seeding to all open rings is done by perfusing the inlet with cell suspension either with a standard pipette or with a syringe pump, the suspension fills the conduits via capillary forces, and with the increasing pressure, droplets start forming beneath the circular grooves. Eventually, pressure equilibrium due to the surface tension at the liquid-air interface, all interconnected droplets will have the same size and volume¹⁵. More recently, H. Kim et al. developed a system for the formation and contact-based transfer of spheroids¹⁶. The system consists of two main parts: a drop array chip (DAC) and a pillar array chip (PAC), both made of PDMS replicas from 3D printed molds, and then attached bonded to glass slides. The DAC has an array of concave wells onto which cell suspension or reagents are pipetted then flipped to form hanging drops or load reagents for fluid exchange, respectively. The PAC has a matching array of truncated, conical pillars with concave apical surfaces for the pick-up and transfer of spheroids from the DAC. After spheroid pick-up, more liquid handling processes can be carried out using other sets of DACs, loaded with the needed reagents (e.g. fresh medium), and repeating the same steps 16.

Each of these platforms improve the process of forming and/or handling hanging drops. Some of them offer the possibility of precise fluidic manipulations via complex microfluidic networks with flow control elements, such as micro-valves and gradient generators. However, some limitations persist. Majority of existing platforms still require a pipetting step into each "hanging drop well" for initial cell seeding, which is laborious if robotics is not accessible or compatible with the platform. Moreover, some platforms jeopardize the practicality of the design when developing devices based on complex microfluidic concepts that require highly skilled personnel to operate and peripheral equipment attached to the system, such as fluid pumps. Not to mention the fine tuning required for key parameters, such as pressure, flow rates, and surface characteristics. Furthermore, the manufacturing process of the platforms often involves multiple molding steps, or specialized instruments.

In this work, we aim to provide an improved hanging drop platform that offers simplicity of manufacturing as well as operation, incorporating useful design features from existing platforms, and further improving certain aspects to make it more user-friendly. The provided solution is 3D printed from a biocompatible material that can be used for cell culture, which decreases post-processing procedures, eliminates the need for moulding steps, and offers higher degrees of design freedom in a cost-effective manner. Moreover, the platform does not require to be attached to bulky specialized equipment, making it more accessible to different labs, and reducing the lab space required to use it. As a proof of concept for cell aggregation, round, compact spheroids of HT29 and MCF-7 were formed, then picked-and-placed as circular arrays on 24-well plate surfaces. By changing the motif of the pick-and-place pillars, different patterns can be generated on well plate surfaces. Patterns of rectangular arrays, circle, and maple leaf

shape were created as a demonstration. The presented platform offers a practical solution to make spheroid production and handling easier.

2.3. Methods

2.3.1. Cell Culture

HT29 colorectal adenocarcinoma cell lines and MCF-7 breast adenocarcinoma cell lines were cultured in RPMI 1640 media supplemented with 10% fetal bovine serum (FBS, Gibco) and 1% penicillin-streptomycin (Thermo Fisher Scientific). All cells were kept in a humidified incubator at 37 °C and 5% CO₂. MCF-7 cells were transfected with GFP. HT29 cells were transfected either with GFP or TdTomato.

2.3.2. System Manufacturing

System components (Figure 1A-H) were designed in SolidWorks (Dassault Systèmes SolidWorks Corporation), exported as "STL" files, then 3D printed using MiiCraft Prime 110 (Creative CADworks, Concord, Canada) with a 385 nm LED. The resin was made of Poly(ethylene glycol) diacrylate (PEGDA, Sigma) with 250 molecular weight mixed with 0.8% w/w Phenylbis(2,4,6-trimethylbenzoyl)phosphine oxide as a photoinitiator (PABO, Sigma) and 0.2% Isopropylthioxanthone (ITX) as a photoabsorber. PEGDA was chosen due to its good biocompatibility, transparency, and surface properties that are favorable for cell culture applications 17–20. After printing, all parts were washed in 70% ethanol, crosslinked with UV light for 2 minutes, then washed again with ethanol for at least 7 days to ensure removal of residual unpolymerized resin.

2.3.3. Spheroid Formation

For droplet formation (Figure 1), aggregation pillars were inked with 1 mL of cell suspension in a 60 mm petri dish. Cell suspension filled the hollow channel inside each pillar via capillary action. Once the liquid reaches the top of the pillar, it stops due to the abrupt change in the geometry of the microchannel forming what is known as a stop valve²¹. At this point, the aggregation pillars are mounted on top of standard 24 well plates filled with autoclaved water for humidification, then plunger-like structures are inserted into the pillar to push the suspension towards the surface of the pillars where the hanging droplets are stably formed. The plate is wrapped with parafilm and incubated in a humidified incubator at 37 °C and 5% CO₂ for 2 days to facilitate aggregation.

Cell suspension in prepared from RPMI supplemented with 1% penicillin-streptomycin (Thermo Fisher Scientific), with or without 10% FBS (Gibco). To enhance aggregation, 0.5% Methylcellulose (MethoCel, Sigma-Aldrich) was added²². Cell density of the suspensions was kept at 50,000 cells/mL.

2.3.4. Spheroid Pick-and-Place

In preparation for spheroid patterning, 24-well plate surfaces were washed with poly-D-lysine (PDL) then coated with 0.1 mg/mL Collagen type I rat tail (Corning). Once cells are aggregated, pick-and-place pillars of matching motif are used to pick-up spheroids from the aggregation pillars, and brought in contact with the well surface to transfer the spheroid. Then, the same pick-and-place pillars are inked with 2% low viscosity ultra-pure alginate (NovaMatrix), and the formed alginate droplets are transferred on top of the previously deposited spheroids. Now that

the spheroids are embedded within alginate droplets, 0.2 M calcium chloride solution (CaCl₂) in TRIS buffer is used for the ionic crosslinking of alginate. This way, the spheroids are confined in their spots. The well is then filled with culture media. Alginate was chosen due its favorable properties for cell culture applications. This include its biocompatibility, porosity, and rapid crosslinking to prevent evaporation of minute volumes²³.

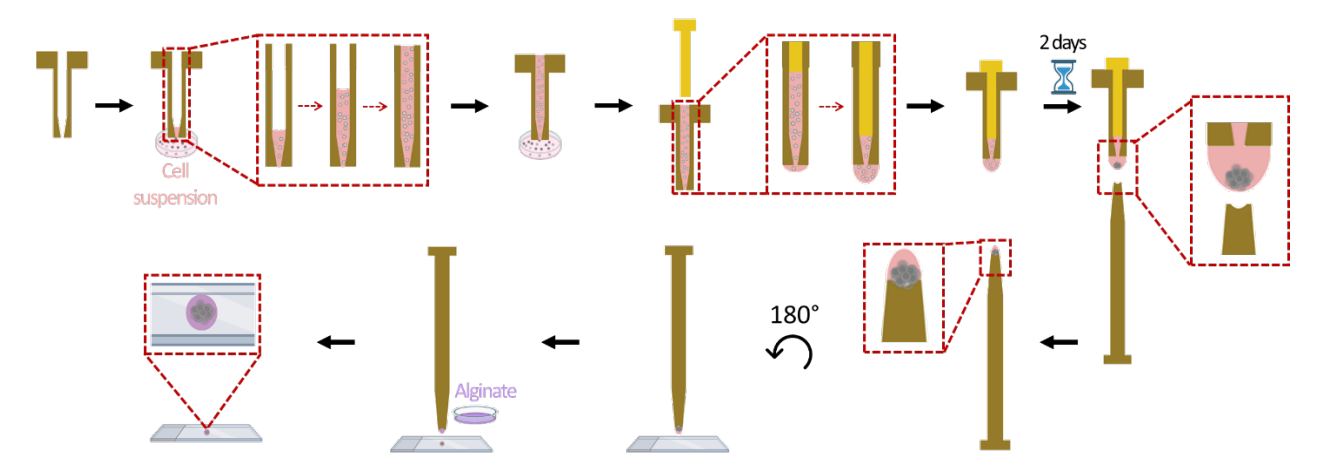


Figure 1. Simplified schematics of the workflow of the system. <u>Top row:</u> the process starts with approaching aggregation pillars with a petri dish filled with cell suspension. Cell suspension fills the hollow channel in the aggregation pillar via capillary action. Once the liquid reaches the top, it stops due to the abrupt change in channel dimensions (stop valve). A plunger is then inserted into the channel to push out the cell suspension forming a droplet at the surface of the pillar. The pillar is then incubated for two days in a humidified environment allowing for gravity-mediated aggregation of cells. <u>Bottom row:</u> once spheroids are formed, the pick-and-place pillars are used to first pickup the suspended spheroid, and then deposit it onto a culture surface. The same pick-and-place pillars are used to deposit a droplet of alginate on top of the spheroid to lock-it in place. Figure created using BioRender. Figure not to scale.

2.3.5. Cytotoxicity Testing

Cytotoxicity tests were conducted in accordance with ISO 10993-12:2012(E) and ISO 10993-5:2009(E). Conditioned media was prepared by incubating cell culture media with 3D printed

PEGDA resin slabs for 24 hours. Slabs UV-crosslinked for 2 minutes, as well as un-crosslinked slabs were used. The slabs were washed in 70% ethanol for 1, 5, or 9 days prior incubating them with media. The surface area of tested material:media volume ratio was 3 cm² per 1 mL of media. The conditioned media was then used to culture HT29 and MCF-7 cell monolayers in 96-well plates at an initial cell seeding density of 10,000 cells/well. Quantitative effect of cyto-toxicity was tested by measuring the metabolic activity of cells with WST-1 assay (Sigma-Aldrich). The mitochondria of metabolically active cells produce dehydrogenases that cleave the tetrazolium salt WST-1 into formazan. Briefly, the WST-1 reagent was added to the wells after 24 hours of culture in conditioned media at a ratio of 1:10 (vol/vol) and incubated for 2-4 hours. Then, the optical density (OD) of formazan was measured at 440 nm with SpectraMax i3 multimode spectrometer (Molecular Devices, California, USA). The background measurement at 640 nm was subtracted measurement. The experiment has positive controls of cells cultured with regular media without any exposure to PEGDA, and negative controls of cells culture with conditioned media from slabs that are not UV-crosslinked nor ethanol washed.

2.3.6. Microscopy and Imaging

Microscopy images were taken with the Eclipse Ti2 confocal microscope and analyzed using NIS-Element (Nikon, Japan). A 4x or 10x air objectives were used for all images. Patterned spot dimeters and spheroid circularity was measured using Fiji software (NIH, USA). Circularity is defined according to the equation below²⁴:

$$Circularity = 4\pi \times \frac{Area}{Perimeter^2}$$
 (1)

A perfect circle has a circularity value of 1, and that value approaches zero as the shape gets more elongated²⁴.

Photographs of the 3D printed parts were taken with a Sony A7RIII camera equipped with a FE 90 mm F2.8 Macro G OSS lens. Extra magnification to image fine structures was achieved using a macro extension tube that reduces the minimum focal distance of the camera. Droplet images were taken with a Panasonic Lumix DMC-GH3K camera.

2.3.7. Droplet Characterization

PBS with blue food color dye, supplemented with 0.5% MethoCel, was used for visualization purposes. Droplet images were analyzed with the contact angle plugin in Fiji software to calculate the angle the droplet forms with the pillar as well as the radius of curvature of the pillar. Droplet volumes were manually measured with a pipette. The evaporation test was conducted by incubating the aggregation pillars loaded with the same PBS solution in a humidified cell culture, while measuring the mass of the droplet after 2, 5, 24, and 48 hours. The measured mass was subtracted from the dry mass of the setup that was measured before starting the experiment.

2.3.8. Data Analysis

Results are reported as mean ± standard deviation. Error bars represent the standard deviation.

2.4. Results and Discussion

2.4.1. System Design and Operation

The developed system consists of two main parts: aggregation pillars (Figure 2) and pick-andplace pillars (Figure 2E-F). Both pillar sets are attached to a base with curved alignment feature that fits into a commercial 24-well plate. The entire system is 3D printed from PEGDA resin. PEGDA has shown good printability, and favourable properties for cell culture applications²⁰. Aggregation pillars are hollow, with open microchannels where cell suspensions are loaded via capillary action (Figure 2I). Once the channel is filled, capillary flow stops due to the abrupt change in the geometry of the microchannel forming a stop valve²¹. Then, plunger-like structures (Figure 2C-D) are inserted into the pillars to push the suspension towards the surface of the pillars where the hanging droplets are stably formed. Aggregation pillars are then mounted on a 24-well plate filled with water for humidification, the lid is closed, and the whole setup is incubated for two days to allow gravity-mediated aggregation of the cells. Once spheroids are formed, the pickand-place pillars come into play. These pillars are used to pick-up the formed spheroids (Figure 2J-K) from the aggregation pillars, with the aid of a part (Figure 2G-H) that aligns the edges of both pillar sets. Then, the same pick-and-place pillars are inked with alginate precursor and transferred on top of the spheroids to lock them in place. The alginate is crosslinked with calcium chloride. This ionic crosslinking method is instantaneous, allowing for rapid gelation of alginate²³. The calcium chloride is then replaced with cell culture media. Simplified schematics for the entire process of aggregation and pick-and-place is illustrated in Figure 1.

Detailed system dimensions are reported in Supplementary Figure 1. In brief, the base is a 25 x 25 mm². Each base has four peripheral pillars that serve as spacers to prevent the droplet bearing pillars from touching the walls of the wells as the part is moving. Since the system is entirely 3D printed, aggregation pillar diameters can be easily altered, resulting in spheroids with different shapes and dimensions. Here, diameters of 1.5, 3, and 6 mm were tested for aggregation. The diameter of the hollow microchannel can also be altered, resulting in the formation of droplets of varying volumes and radii of curvature, which eventually affects the formed spheroids. The

plunger is designed to have a diameter that is 50 µm less than that of the microchannel, to ensure tight fit and prevent liquid evaporation. For the pick-and-place pillars, smaller diameters are desirable to give smaller pattern spots, and hence, more precision. However, PEGDA pillars smaller than 1.5 mm diameter were brittle making them not practical to work with. Therefore, the pick-and-place pillars were designed to have a diameter of 1.5 mm, with a conical tip where the diameter is reduced to 0.4 mm. This way, the pillar is stable, and the tip is small enough to allow for precise patterning. The tip surface has a hollow hemisphere with 0.55 mm diameter in the middle acting as mini-cup to pick-up the spheroid. Air vents are added to enhance the efficiency spheroid pick-up by preventing air entrapment in the hemisphere.

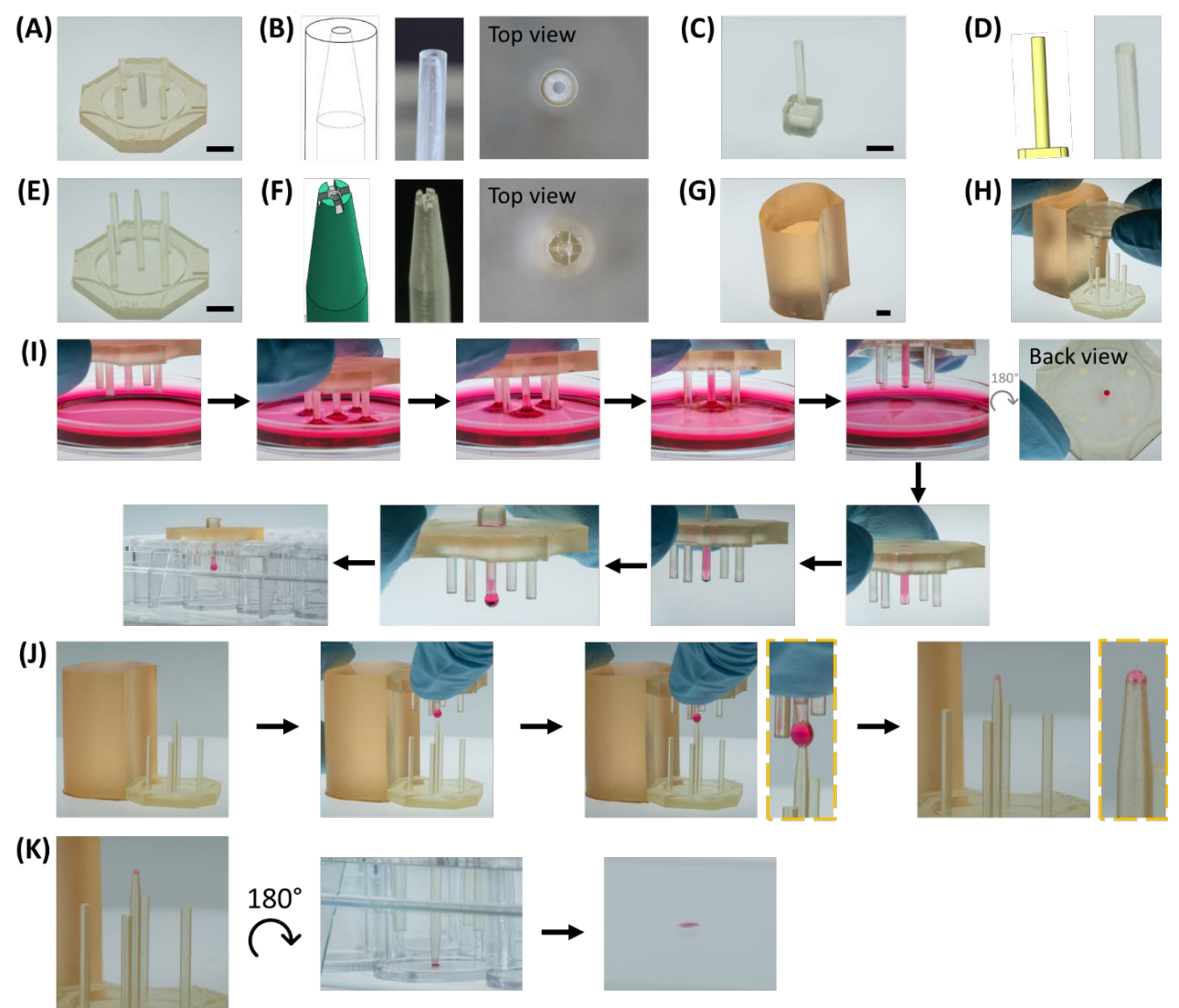


Figure 2. The system and the workflow. (A) Photograph of an aggregation part with one aggregation pillar in the middle, and four periphery spacer pillars. Parts with pillar is shown throughout this figure to clarify the concept with well-focused images. (B) Zoomed-in CAD drawing (left), side view picture (middle), and top view picture (right) of the aggregation pillar in A. (C) Picture of the plunger used to push put the cell suspension in the hollow channel of the aggregation pillar. (D) CAD drawing (left) and a zoomed-in picture of the plunger (right). (E) Photograph of a pick-and-place part with one pick-and-place pillar in the middle, and four periphery spacer pillars. (F) Zoomed-in CAD drawing (left), side view picture (middle), and top view picture (right) of the pick-and-place pillar in E. (G) Alignment part that is used to align both pillar sets during the pickup process (H). Pillar sets shown in A and E are connected to a 25 x 25 mm²

base that has curved alignment features to fit within 24-well plates. The surface of the base can be used to engrave text that identifies each part. (I) Pictures for the process of droplet formation using colored PBS to visualize. The process starts with dipping the aggregation pillar in a petri dish filled with suspension, the hollow channel in the aggregation pillar will start to fill via capillary forces until it fills it completely. Liquid flow stops due to the abrupt change in geometry forming a stop valve (as seen in the back view). Then, the plunger is inserted in the hollow channel to push the liquid out, and form a droplet at the surface of the pillar. The aggregation pillar is then mounted onto a 24-well and incubated for gravity mediated spheroid formation. (J) Pictures for the process of droplet pickup. The pick-and-place pillar is place facing up, then it is aligned with the aggregation pillar using the alignment part. The formed droplet is brought in contact with the tip of the pick-and-place pillar (zoomed-in image at the time of contact in the yellow frame). Upon contact, the spheroid situated at the center of the curvature of the droplet will be transferred to the pick-and-place pillar. The latter is the flipped 180° (K) and brought in contact with a 24-well plate surface to transfer the spheroid. Scale bars = 1 cm.

2.4.2. System Biocompatibility

Before using the system for spheroid formation, we needed to ensure that the material used in 3D printing, i.e. PEGDA, is cytocompatible with the two cell lines used in this study. To do so, we 3D printed slabs of PEGDA and applied different post-processing protocols, including crosslinking PEGDA with UV, and washing in ethanol for 1, 5, or 9 days to wash away any unpolymerized resin (Figure 3). The slabs were incubated in cell culture media that was then used to culture HT29 and MCF-7 cells in 96-well plates for a day. After that, we measured the metabolic activity of the cells using the WST-1 assay.

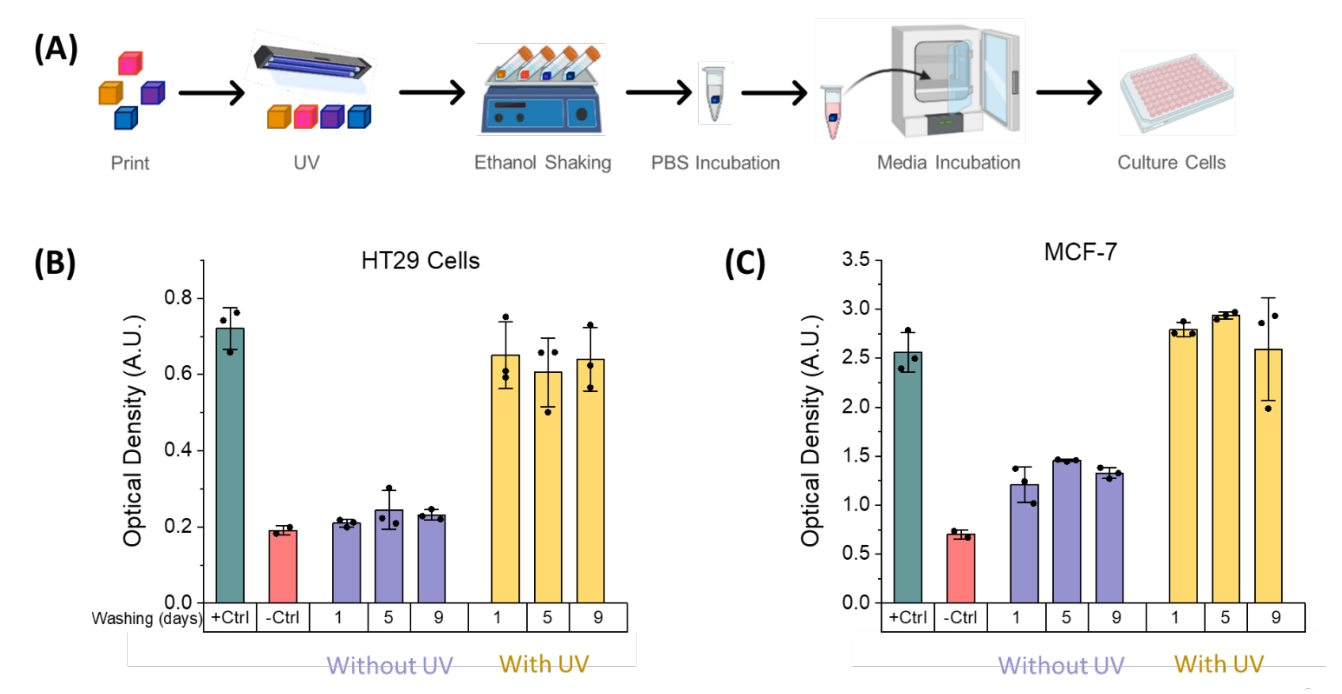


Figure 3. Cytotoxicity test of PEGDA. (A) Schematics summarizing the protocol followed for cytotoxicity testing. (B) Metabolic activity of HT29 cells cultured with conditioned media from varying PEGDA UV crosslinking and ethanol washing durations. (C) Metabolic activity of MCF-7 cells cultured with conditioned media from varying PEGDA UV crosslinking and ethanol washing durations. Schematics in A were created with Biorender.

For both cell lines, our results show that UV crosslinking is vital for making PEGDA cytocompatible. Washing with ethanol alone, even for 9 days, was not enough to get rid of toxic resin residuals. However, 2 minutes of UV crosslinking in conjunction with a day of ethanol washing resulted in cell metabolism comparable to that of the positive control. Additional days of ethanol washing did not have a significant effect on the metabolic activity of cells.

2.4.3. Characterization and Cell Culture Optimization

After optimizing the protocol for PEGDA post-processing, we proceeded to optimize the culture conditions for spheroid formation. We challenged the system to form HT29 and MCF-7 spheroids. The former is known to form tight spheroids, while the latter typically forms more loose

aggregates²⁵. For this set of experiments, in order to examine the effect of culture conditions on a single spheroid, a simplified the system with one aggregation pillar per part, and one pick-and-place pillar was used.

When attempting to form spheroids with cell suspension without any additives, HT29 cells failed to form compact spheroids. The resulting aggregates had irregular, elongated shapes with an average aspect ratio of 1.4 ± 0.4. Moreover, the aggregates had a more flat morphology rather than a truly 3D spherical shape (Figure 4). The average length in the Z direction of confocal images in this group was 67.7 ± 13 µm. This is a common problem in spheroid making protocol. It is suggested that media additives could overcome this limitation by altering the rheological properties of the cell suspension and creating a crowding effect that helps with cell aggregation²². Since the patterning process in our system utilizes alginate, we first tested if it can as well improve spheroid formation. Contrary to our expectations, supplementing cell suspensions with 2% alginate resulted in small, flat, and dispersed cell clumps. It has been reported the G-block of alginate induce physical stress on cells and could lead to apoptosis³⁷. We then tested the effect of adding MethoCel to the suspension. MethoCel is commonly used as an inert, biocompatible additive in spheroid formation protocols. Our results show that supplementing the suspension media with 0.5% MethoCel noticeably enhances the formation of compact HT29 spheroids, and was adopted as the standard for all subsequent cell experiments in this work. While the exact mechanism by which MethoCel acts is largely unknown, it is attributed to its viscosity and induction of a crowding effect that helps cells aggregate together²². Similarly, MCF-7 cells failed to form spheroids with media without additives or media supplemented with alginate (Figure 4).

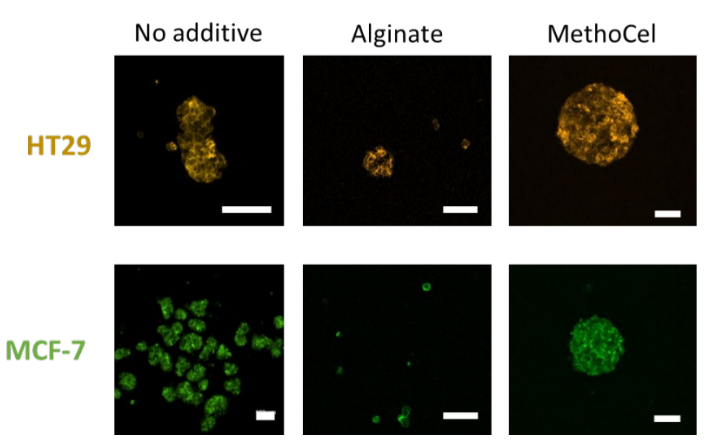


Figure 4. Effect of media additives on aggregating HT29 and MCF-7 cells using the developed system. Scale bars = $100 \mu m$

After optimizing the aggregation medium composition, we tested the effect of modulating aggregation pillar dimensions. It is speculated that smaller overall pillar diameters will result in more compact spheroids, and larger diameters with results in more spread out aggregates. To test this, we printed aggregation pillars with diameters of 1.5, 3, and 6 mm. We also tried larger than 6 mm, however, the resulting droplet from that pillar was flat, with no room for cells to aggregate (data not shown). HT29 spheroids formed with 1.5 mm pillars were round, dense, and compact with an average circularity index of 0.96 (Figure 5) as defined by equation (1). Spheroids formed with 3 mm pillars were smaller in size, but still round and compact with an average circularity index of 0.93. Spheroids formed with 6 mm pillars had more elongated shapes with an average circularity index of 0.81. Increasing pillar diameters also resulted in forming flatter spheroids. The average length in the Z direction for HT29 spheroids was 139.6 ± 29 μm, 112.2 ± 3 μm, and 81.7 ± 40 μm for the 1.5, 3, and 6 mm diameter pillars, respectively. For MCF-7, circularity was significantly less regardless of pillar diameter, as all spheroids had irregular shapes rather than round spheres (Figure 5B). However, similar to HT29 spheroids, MCF-7 did become more flat with increasing pillar diameters. The average length in the Z direction for MCF-7 spheroids was $223.7 \pm 17 \,\mu\text{m}$, $168.9 \pm 16 \,\mu\text{m}$, and $156.9 \pm 85 \,\mu\text{m}$ for the 1.5, 3, and 6 mm diameter pillars, respectively. As speculated, smaller pillar diameters are favorable for forming spheroids. Therefore, pillars of 1.5 mm diameter were printed for all subsequent experiments.

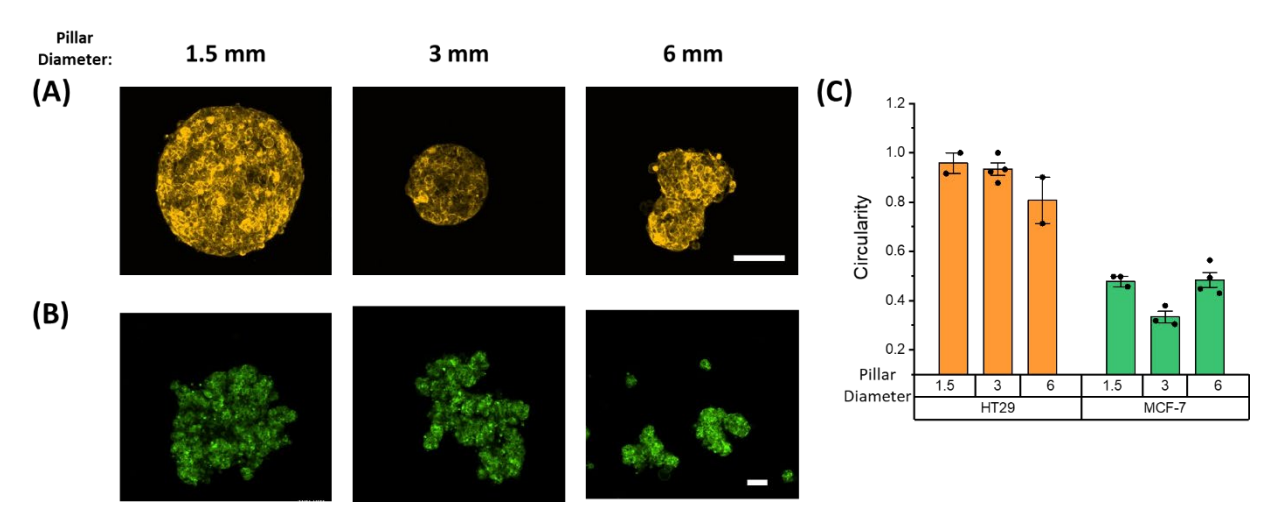


Figure 5. Effect of changing aggregation pillar diameters on (A) HT29, and (B) MCF-7 spheroids. Figure showing maximal intensity projections of confocal images. Scale bars = 100 μ m. (C) Bar charts comparing the circularity of resulting spheroids as define in equation (1) in section 2.3.6.

The dimension of the hollow channel in the aggregation pillar also has an effect on the shape and volume of the formed droplets. To optimize the diameter of the hollow channel, we characterized the droplets formed by different channel diameters. Testing was done with dyed PBS supplemented with 0.5% MethoCel for visualization purposes. Aggregation pillars of 1.5 mm with hollow channel diameters of 0.6, 0.8, and 1 mm were used in this set of experiments (Figure 6). Higher media volumes are desirable for the HDT since it gives more nutrients to the cells as they aggregate. Droplet volumes were $1.7 \pm 0.3~\mu$ L, $5.3 \pm 1~\mu$ L, and $7.3 \pm 1~\mu$ L for aggregation pillars of 1.5 mm with microchannel diameters of 0.6, 0.8, and 1 mm, respectively (Figure 6A). Discrepancies between the theoretical droplet volume calculated from the hollow channel dimensions and the experimental volume could be attributed to differences in the printed

dimensions as well as potential minor droplet evaporation. Moreover, the shape of the droplet at the liquid-air interface influences the shape of the formed spheroids. The lower the radius of curvature is, the rounder the interface is. Volume of the droplet is maximized when the droplet forms a right angle with the pillar. At this point, the radius of curvature of the droplet is lowest. Our data show that hollow channel diameters of 0.8 and 1 mm result in droplets with angles close to 90° with the pillars, and the least radii of curvature compared to the 0.6 mm channel diameter. Droplets generated from the 0.6 mm microchannel formed acute angles with the pillars, and had a slightly higher radii of curvature (Figure 6B-C). Based on these results, the 1 mm microchannel diameter gives a good droplet volume with a favourable droplet shape at the liquid-air interface. Therefore, it was adopted for all aggregation pillars used in this work. Notably, despite the droplets having relatively small volumes, the composition of the liquid in conjunction with the humidification in the 24-well plate setup results in minimal evaporation over the two days duration used to aggregate cells (Figure 6D).

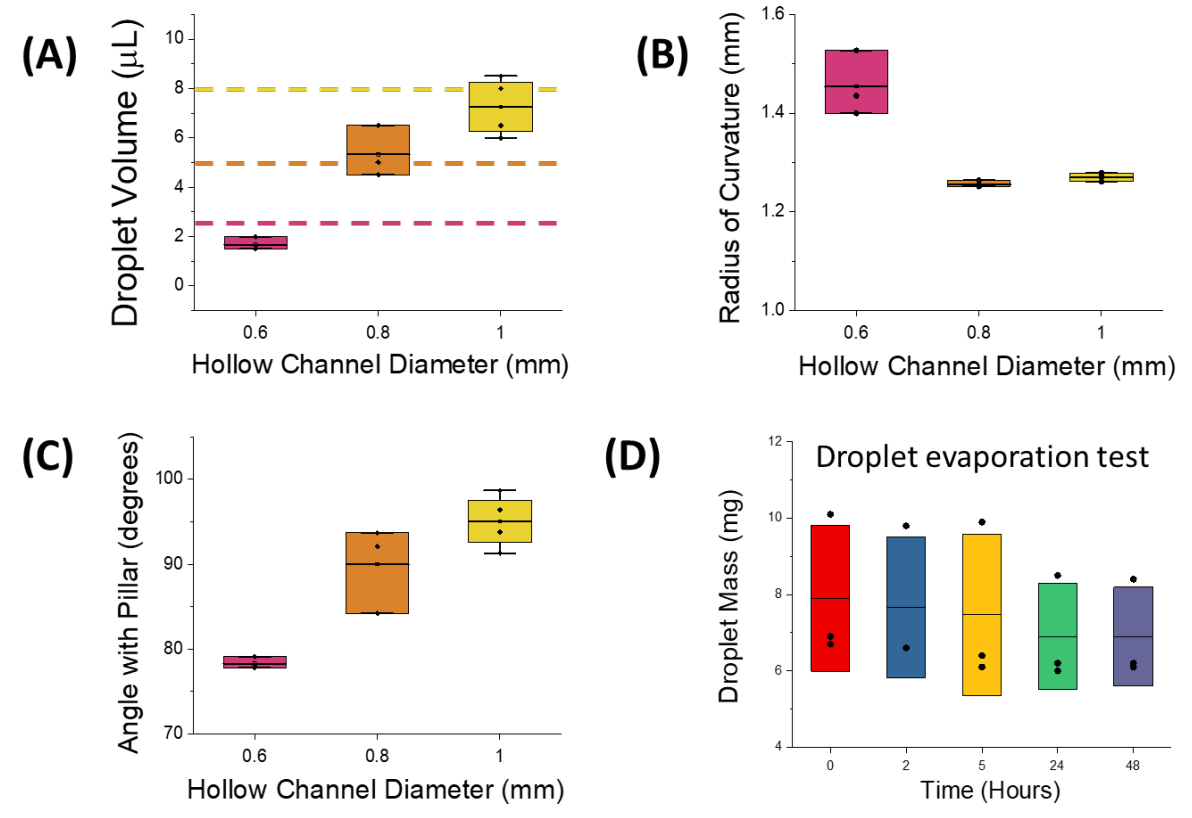


Figure 6. Optimizing hollow channel diameter in aggregation pillars of fixed 1.5 mm diameter. (A) Quantification of droplet volumes when varying hollow channel diameter. Dashed lines indicate the theoretical volume based on hollow channel dimensions. (B) Quantification of the radii of curvature of the formed droplets. (C) Quantification of the angles between formed droplets and the pillars. (D) Droplet mass measured over two days to test droplet evaporation.

2.4.4. Patterning and Proof-of-Concept

As a proof-of-concept, the system was used to create circular and square patterns on 24-well plate surfaces (Figure 7A). More complex pattern can also be created by simply drawing the motif of the desired shape with the pick-and-place pillars. As an example, we created a pattern for the Canadian maple leaf. In order to define the maple leaf shape, droplets had to be deposited in close proximity to one another, resulting in alginate droplets to get partially mixed prior crosslinking. Moreover, alginate droplets spread on the collagen coated well plate surface

beyond the diameter of the tip of the pick-and-place pillar. For all proof-of-concept experiments except the maple leaf shape, the system was used for the parallel transfer of patterns created with the pillar sets. Serial transfer was partially tested to generate the maple leaf pattern where three pick-and-place parts were sequentially stamped on a 24-well to create the maple leaf shape. While the overall shape shows the intended pattern, mixing between adjacent spots is unavoidable. CAD images of the pick-and-place pillars for all patterns shown in Figure 7A are provided in Supplementary Figure 2. Future work can focus on serially transferring two or more different arrays that would then overlap potentially creating complex patterns achieved with microarraying instruments.

In fact, quantification of the patterned spot diameter shows that it is nearly double the diameter of the deposition tip. The tip diameter is 0.4 mm, while the average spot diameter is 0.89 \pm 0.13 mm (n = 70). The relatively small standard deviation reflects the consistency of the process and reproducibility of the system. Spot diameter was consistent across different patterns created with different parts. Furthermore, the accuracy and precision of the system in creating patterns was validated by measuring the deviation between the theoretical position of the spheroids, which is at the center of each pillar, and the actual position within the patterned array (Figure 7C). The average deviation is $159 \, \mu m \pm 138 \, \mu m$, with a deviation range between 0 and 430 $\, \mu m$ (n = 16). Knowing that average spheroid diameter is $317 \pm 28 \, \mu m$, the misalignment is within half a diameter in relation to the spheroids. Higher deviations, when they occur, could be attributed to spheroid movement within the patterned spot before alginate gelation. Pre-wetting the surface with a thin liquid film may help in limiting the movement of the spheroid upon deposition, and therefore enhance positional accuracy.

After all system optimizations and characterization, we tested it for making circular HT29 spheroid arrays (Figure 7D). The success rate of pick-and-place of spheroids was 72% (n = 3). In some instances, air entrapment or clogging in the hemisphere at the tip of pick-and-place pillar could prevent efficient spheroid pickup. Moreover, it is possible that some variability in the size of the hanging droplets on the aggregation pillars prevent all of them to contact the pick-andplace pillars for spheroid transfer at the same time, resulting in leaving some spheroids without pick-up. In a related context, small tilting in the two pillar sets, aggregation and pick-and-place, during spheroid transfer process could shift the location of spheroids off the center of the pillars. This would result in spheroids not picked-up from the aggregation pillars, or not deposited during the pattern transfer step. Hence, the alignment part was added to the setup, and it did contribute to enhancing the success rate by 50%. To enhance spheroid patterning success rate, an error correction feature can be implemented in the system by designing single pillars to selectively transfer spheroids to the targeted spots that were missed in the initial pattern transfer step. Alternatively, a more specialized, and more costly option would be to use automated inkjet spotters, if available, to scan the well for missing spots, and re-deposit spheroids where required. It is practically not feasible to achieve this level of accuracy and precision in deposition of patterns in manual spheroid transfer methods due to several reasons. Hand tremors can result in deposition that is off-location by several millimetre. Furthermore, the confined deposition spot is attributed to the small diameter of the pick-and-place pillar tip as well as the minute media volume carried when picking up the spheroid. Using a pipette tip for example would result in larger spots. Moreover, the alignment features on the pick-and-place pillars base ensure that the

droplet is perpendicular to the well plate surface at the time of spheroid transfer, resulting in more consistent deposition that is very hard to achieve if depositing by hand with a pipette.

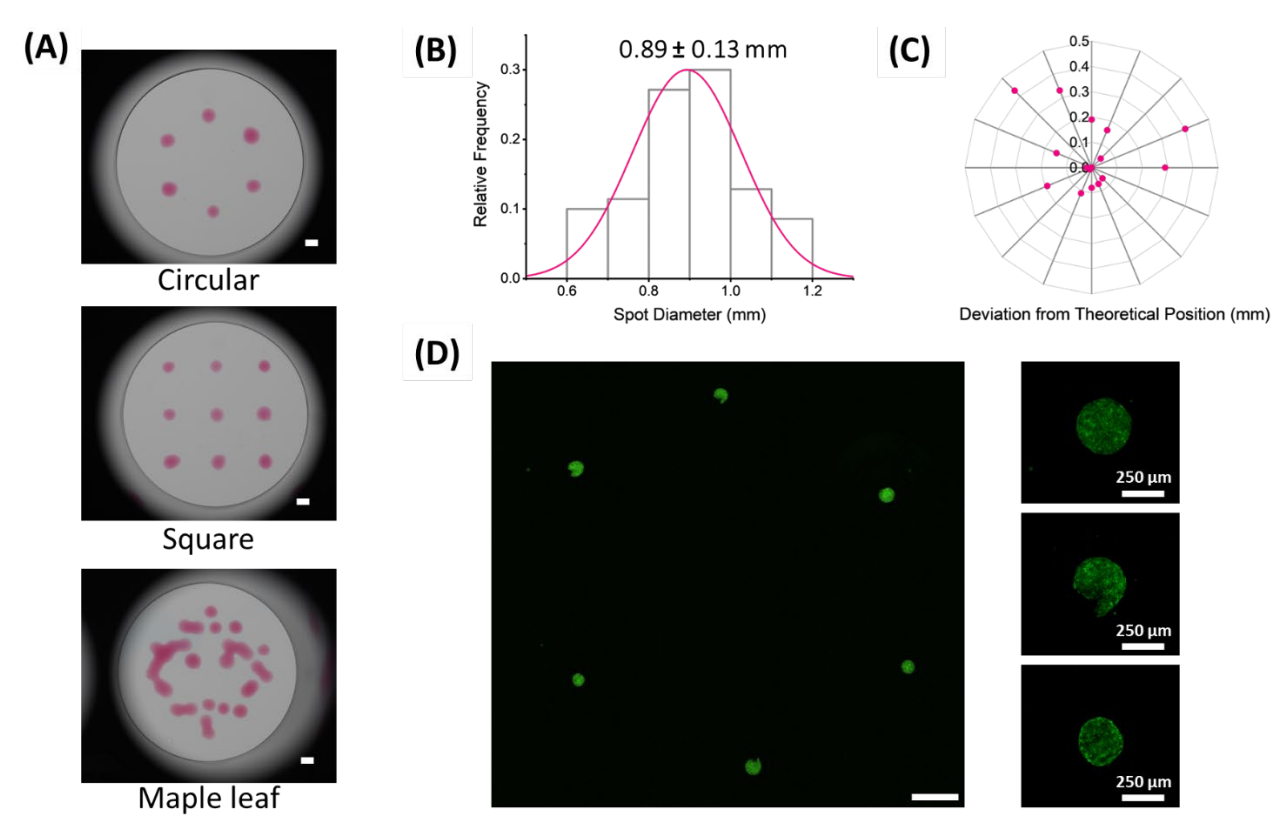


Figure 7. Patterning and Proof-of-Concept. (A) Circular, square, and maple leaf alginate patterns formed using the system. Pink food color dye was added to the alginate hydrogel for visualization purposes. (B) Histogram showing the distribution of patterned spot diameters from all patterns (n = 70). (C) A scatter plot of the deviations between the theoretical spheroid position (in the CAD design) and the actual spheroid position in the array pattern as a measure of patterning accuracy and precision (n = 16). (D) Proof-of-concept HT29 spheroids circular array. On the right, zoomedin, maximal intensity projections of three spheroids in the pattern. Scale bars are 1 mm unless otherwise stated.

2.5. Conclusion

In conclusion, we developed a hanging drop system for the production and precise positioning of spheroids. The system is entirely 3D printed from biocompatible resin and can be used for cell

culture purposes after minimal post-processing steps. Moreover, the system is compatible with commercial 24-well plates, making it easy to adopt in most labs. By modulating simple dimensions, the size and shape of produced spheroids can be altered. As a proof of concept, the system was used to aggregate HT29 and MCF-7 cell lines, create different patterns, and create circular arrays of HT29 spheroids. Future work will focus on design enhancements to improve spheroid pick-up efficiency, improvement of the alignment features to allow for better precision in spheroid deposition, testing for the aggregation of more cell types, as well as increase the throughput of aggregation and patterning.

2.6. Acknowledgements

The authors would like to thank Molly Shen for providing the fluorescently labelled cell lines used in this work, and Yonatan Morocz for helping with taking the setup photographs in Figure 2. The authors would also like to thank Prof. Maryam Tabrizian for giving them access to the plate reader for WST-1 absorbance measurements.

2.7. References

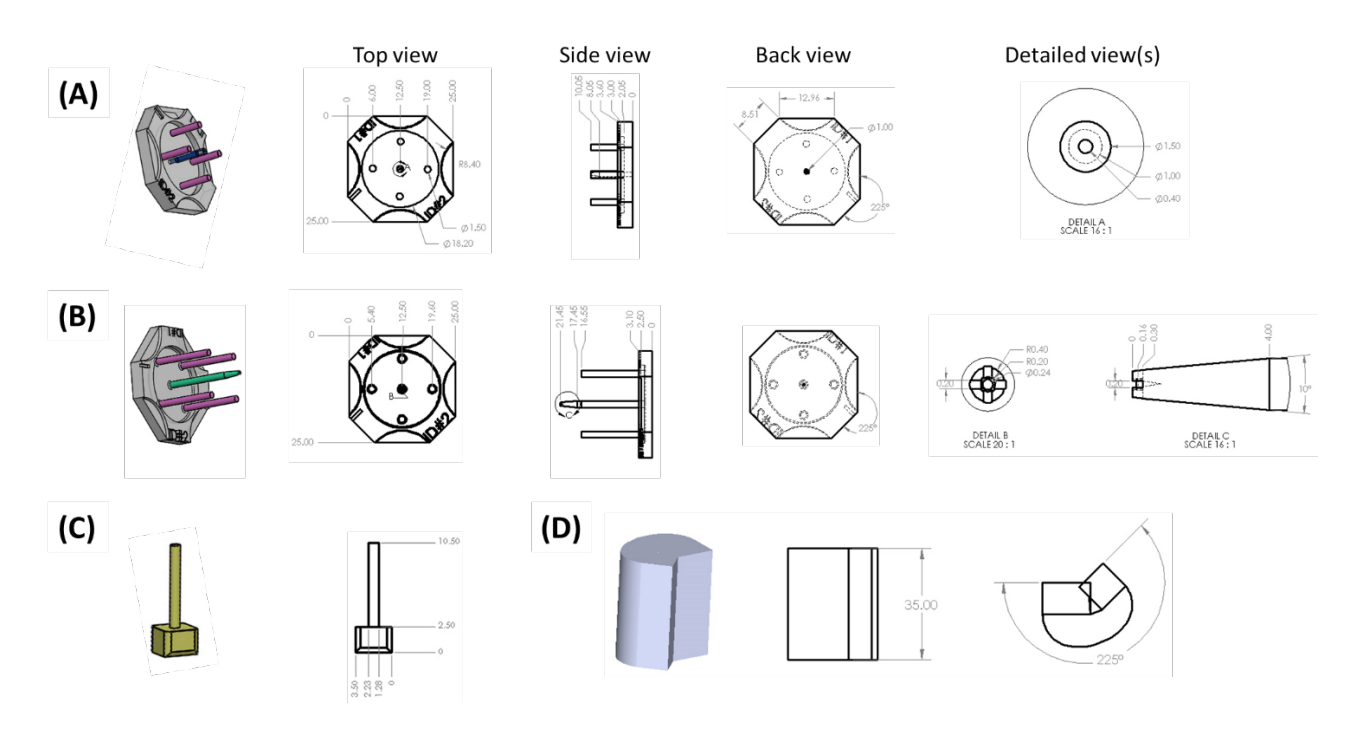
- 1. Mohs, R. C. & Greig, N. H. Drug discovery and development: Role of basic biological research. *Alzheimers Dement. Transl. Res. Clin. Interv.* **3**, 651–657 (2017).
- 2. Kraljevic, S., Stambrook, P. J. & Pavelic, K. Accelerating drug discovery. *EMBO Rep.* **5**, 837–842 (2004).
- 3. Donowitz, M., Turner, J. R., Verkman, A. S. & Zachos, N. C. Current and potential future applications of human stem cell models in drug development. *J. Clin. Invest.* **130**, 3342–3344 (2020).

- 4. Velasco, V., Shariati, S. A. & Esfandyarpour, R. Microtechnology-based methods for organoid models. *Microsyst. Nanoeng.* **6**, 1–13 (2020).
- 5. Jensen, C. & Teng, Y. Is It Time to Start Transitioning From 2D to 3D Cell Culture? *Front. Mol. Biosci.* **7**, (2020).
- 6. Hsu, S.-H. & Hsieh, P.-S. Self-assembled adult adipose-derived stem cell spheroids combined with biomaterials promote wound healing in a rat skin repair model. *Wound Repair Regen. Off.*Publ. Wound Heal. Soc. Eur. Tissue Repair Soc. 23, 57–64 (2015).
- 7. Kawaguchi, S. *et al.* Intramyocardial Transplantation of Human iPS Cell–Derived Cardiac Spheroids Improves Cardiac Function in Heart Failure Animals. *JACC Basic Transl. Sci.* **6**, 239–254 (2021).
- 8. Wu, Y. C. *et al.* Transplantation of 3D adipose-derived stem cell/hepatocyte spheroids alleviates chronic hepatic damage in a rat model of thioacetamide-induced liver cirrhosis. *Sci. Rep.* **12**, 1227 (2022).
- 9. Gunti, S., Hoke, A. T. K., Vu, K. P. & London, N. R. Organoid and Spheroid Tumor Models: Techniques and Applications. *Cancers* **13**, 874 (2021).
- 10. Langhans, S. A. Three-Dimensional in Vitro Cell Culture Models in Drug Discovery and Drug Repositioning. *Front. Pharmacol.* **9**, 6 (2018).
- 11. Pinto, B., Henriques, A. C., Silva, P. M. A. & Bousbaa, H. Three-Dimensional Spheroids as In Vitro Preclinical Models for Cancer Research. *Pharmaceutics* **12**, 1186 (2020).
- 12. Nath, S. & Devi, G. R. Three-Dimensional Culture Systems in Cancer Research: Focus on Tumor Spheroid Model. *Pharmacol. Ther.* **163**, 94–108 (2016).

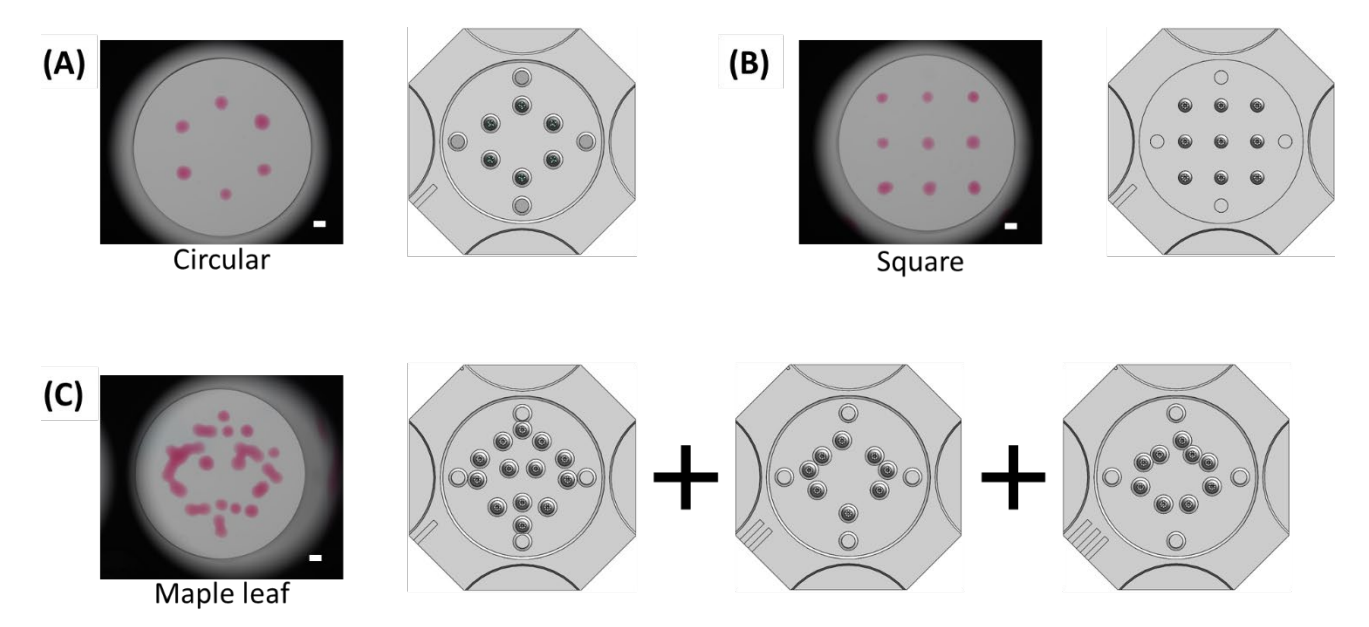
- 13. Gao, B., Jing, C., Ng, K., Pingguan-Murphy, B. & Yang, Q. Fabrication of three-dimensional islet models by the geometry-controlled hanging-drop method. *Acta Mech. Sin.* **35**, 329–337 (2019).
- 14. Tung, Y.-C. *et al.* High-throughput 3D spheroid culture and drug testing using a 384 hanging drop array. *The Analyst* **136**, 473–478 (2011).
- 15. Frey, O., Misun, P. M., Fluri, D. A., Hengstler, J. G. & Hierlemann, A. Reconfigurable microfluidic hanging drop network for multi-tissue interaction and analysis. *Nat. Commun.* **5**, 4250 (2014).
- 16. Kim, H., Roh, H., Kim, H. & Park, J.-K. Droplet contact-based spheroid transfer technique as a multi-step assay tool for spheroid arrays. *Lab. Chip* **21**, 4155–4165 (2021).
- 17. Urrios, A. *et al.* 3D-printing of transparent bio-microfluidic devices in PEG-DA. *Lab. Chip* **16**, 2287–2294 (2016).
- 18. Biocompatible PEGDA Resin for 3D Printing. ACS Appl. Bio Mater.
- 19. Peter, M. & Tayalia, P. An alternative technique for patterning cells on poly(ethylene glycol) diacrylate hydrogels. *RSC Adv.* **6**, 40878–40885 (2016).
- 20. Karamzadeh, V., Sohrabi-Kashani, A., Shen, M. & Juncker, D. Digital Manufacturing of Functional Ready-to-Use Microfluidic Systems. *Adv. Mater.* **n/a**, 2303867.
- 21. Olanrewaju, A., Beaugrand, M., Yafia, M. & Juncker, D. Capillary microfluidics in microchannels: from microfluidic networks to capillaric circuits. *Lab. Chip* **18**, 2323–2347 (2018).

- 22. Leung, B. M., Lesher-Perez, S. C., Matsuoka, T., Moraes, C. & Takayama, S. Media additives to promote spheroid circularity and compactness in hanging drop platform. *Biomater. Sci.* **3**, 336–344 (2015).
- 23. Andersen, T., Auk-Emblem, P. & Dornish, M. 3D Cell Culture in Alginate Hydrogels. *Microarrays* **4**, 133–161 (2015).
- 24. Circularity. https://imagej.nih.gov/ij/plugins/circularity.html.
- 25. Gheytanchi, E. *et al.* Morphological and molecular characteristics of spheroid formation in HT-29 and Caco-2 colorectal cancer cell lines. *Cancer Cell Int.* **21**, 204 (2021).

2.1. Supplementary Information



Supplementary Figure 1. SolidWorks drawings annotated with dimensions of all system components: (A) aggregation pillar, (B) pick-and-place pillar, (C) plunger, and (D) alignment piece. All dimensions are in mm.



Supplementary Figure 2. Top view for SolidWorks drawings of pick-and-place pillars used to create all patterns shown on Figure 7. (A) circular pattern, (B) square pattern, (C) maple leaf pattern. For A and B, parallel transfer for all pattern was used. For (C) sequential transfer for 3 patterns was used to create the maple leaf shape. All dimensions are in mm. Scale bars are 1 mm.

3. Chapter 3: Discussion

The past few decades witnessed a growing need for advanced tools and techniques to create spheroids as valuable in vitro tumor models for different life sciences applications. This demand stems from a collective recognition of the limitations inherent in traditional 2D cell culture systems, which fail to accurately recapitulate the intricate 3D architecture and microenvironment of tissues and tumors in vivo. Spheroids, which faithfully mimic the complex cellular interactions, gradients of nutrients, oxygen, and signaling molecules, offer a promising avenue for more accurate and relevant experimental platforms. These models enable researchers to delve deeper into the understanding of diseases, drug responses, and therapeutic interventions, thereby accelerating drug discovery and development processes. Furthermore, the advent of innovative bioprinting, microfluidics, and biomaterials technologies paved the way for the creation of increasingly sophisticated and customizable spheroids models, allowing researchers to tailor experimental conditions with unprecedented precision. This work utilizes the realm of 3D printing and suspended microfluidics to develop a tool for hanging drop spheroid formation and subsequent pick-and-place of these spheroids into culture surfaces according to pre-determined patterns.

3D printing makes it easy to alter certain system features for user-specific applications. For example, our results show that aggregation pillar diameters can be tuned to control the size and shape of formed spheroids. In general, the smaller the diameter of the aggregation pillar, the rounder and more compact the resulting spheroid is. The smallest stable pillar diameter we could achieve was 1.5 mm. Similarly, the motif of pick-and-place pillars can be modified to generate different patterns; circular, square, and a maple leaf patterns were shown as demonstration.

Smaller pick-and-place pillar diameters are also desirable to decrease the spot size of the pattern, allowing for the creation of denser arrays with high precision. Smaller diameters are possible to print, however, they are more susceptible to breaking during routine handling. This problem also limits the diameter of the plunger. For a 1 mm diameter microchannel in the aggregation pillar, a plunger with a diameter of 0.95 mm is needed. Excess plungers were printed before each experiment as a backup for the ones that break.

To tackle this limitation, a number of techniques may be beneficial. The rigidity of PEGDA-based materials is often influenced by the degree of crosslinking. Higher crosslinking density generally leads to increased rigidity. Decreasing or eliminating the UV crosslinking step after printing could make the material less brittle. Alternatively, reducing the exposure time during 3D printing could also help achieve more flexible PEGDA parts. In addition, blending PEGDA with more flexible polymers, like poly(octamethylene maleate (anhydride) citrate) (POMaC), can help make the material less stiff³². Another method to decrease PEGDA brittleness is to add medical grade, biocompatible plasticizers to the formulation. Plasticizers are additives that can increase the flexibility and reduce the rigidity of polymers³³. To our knowledge, there is no material till date that utilized such additives to enhance PEGDA properties for 3D printing. Future advances in the field may make it possible to have PEGDA resins with higher flexibility that would allow printing stable small pillar diameters.

On a different note, a 3D printer with a 385 nm LED was used since the design has intricate features and hollow microstructures that need to be printed with high resolution. Examples of such features are the hollow microchannel in the aggregation pillars and the hollow hemisphere and air vents in the pick-and-place pillars. 3D printers that use 385 nm LED are generally more

expensive than average consumer-grade printers. They are often used in applications that require high-detail and precision, such as dental, jewelry, and microfabrication industries. Moreover, compared to 405 nm LED printers, 385 nm ones are compatible with a wider range of photoabsorbers to be used in resin formulation, giving a better control over UV light penetration depth and resin polymerization in the z-axis³⁴. On the other hand, printers with 405 nm LEDs are commonly available at more competitive prices. The rapid advances in 3D printing technology may make it possible to achieve similar resolution of 385 nm LED printer with lower cost, benchtop printers.

A major advantage of using PEGDA in this study is its biocompatibility, making the material ready to be used with minimal post-processing steps. While it is important to ensure the cytocompatibility of PEGDA with the specific cell lines used, in our system, the cells are suspended and not directly cultured on the material. Therefore, a conditioned media test following standard ISO 10993-12:2012(E) and ISO 10993-5:2009(E) protocols was sufficient. Applications that require cells to be in direct contact with the material or to adhere to the surface will likely require more stringent post-processing steps and surface coating with cell-adhesive proteins, like collagen, fibronectin, or Matrigel to promote cell attachment and spreading³⁵.

When it comes to patterning using the developed system, our results showed a 100% success rate and reproducibility when patterning alginate droplet, while the success rate for patterning spheroids dropped to 72%. This could be potentially attributed to several factors. Invisible air entrapment or clogging in the tip of the pick-and-place pillars could hinder efficient spheroid pick-up. Moreover, it is possible that some variability in the size of the hanging droplets on the aggregation pillars prevent all of them to contact the pick-and-place pillars for spheroid transfer

at the same time, resulting in leaving some spheroids without pick-up. In a related context, small tilting in the two pillar sets, aggregation and pick-and-place, during spheroid transfer process could shift the location of spheroids off the center of the pillars. This would result in spheroids not picked-up from the aggregation pillars, or not deposited during the pattern transfer step. To enhance spheroid patterning success rate, thorough cleaning of the pick-and-place pillars can be done before each pick-up or transfer step to ensure there is no clogging. Moreover, flat alignment features between the two pillar sets can be designed to guide the contact and ensure the spheroids are centered throughout the whole process. Furthermore, an error correction feature can be implemented in the system by designing single pillars to selectively transfer spheroids to the targeted spots that were missed in the initial pattern transfer step. Alternatively, a more specialized, and more costly option would be to use automated inkjet spotters, if available, to scan the well for missing spots, and re-deposit spheroids where required.

For cell aggregation, our results show poor spheroid formation when media without additives is used. This is not uncommon in literature, as media additives are frequently used to alter the rheological properties of the cell suspension and create a crowding effect that helps with cell aggregation³⁶. Using alginate as a media additive also failed to generate HT29 or MCF-7 spheroids. It has been reported the G-block of alginate induces physical stress on cells and could lead to apoptosis³⁷. Instead, MethoCel was used as an alternative. MethoCel is a chemical compound derived from cellulose, which is a naturally occurring polymer found in plant cell walls. It is inherently biocompatible, and has been used as a thickening agent, stabilizer, and emulsifier in the food and cosmetic industries³⁸. As a media additive, the exact mechanism by which MethoCel acts is largely unknown, but it is speculated that its viscosity and induction of a

crowding effect is what helps cells aggregate together³⁶. Moreover, MethoCel has water-retaining properties, making it useful in preventing evaporation³⁸. Several reported protocols used higher concentrations of MethoCel for the HDT 36,38 , however, our results show that 0.5% MethoCel (v/v) is sufficient to produce round, compact spheroids.

In this work, spheroid arrays with one cell type were created as a proof-of-concept. However, the developed system opens the door for creating more complex arrays of multiple cell types by simply depositing patterns that complement each other in a single well. For instance, one patterning step could be used to deposit an array of cancer spheroids, and the other to deposit liver spheroids in adjacent spots. The crosstalk between the two cell types can be studied with proteomics analysis or microscopy. If spheroids are needed for further analysis after culture, alginate can be digested with alginate lyase, and spheroids can be easily accessible given that they are cultured in standard well plates.

3.1. Future Perspectives

The research presented in this thesis opens promising avenues for future exploration and development in the realm of 3D printing and tissue engineering. One prospective direction involves enhancing the biocompatibility and versatility of the printed tools to accommodate a broader range of cell types and biomaterials, thereby expanding their applicability across various tissue engineering domains. Investigating the scalability and reproducibility of the process is also pivotal to facilitate potential clinical translation in personalized medicine applications, ensuring the feasibility of producing spheroids on a larger scale without compromising their quality. Additionally, modifying the design to support imaging of the aggregation pillars may offer deeper

insights into the dynamics of cell aggregation, aiding in the optimization of key design parameters.

4. Chapter 4: Conclusion

In conclusion, a modified hanging drop system for the production and precise positioning of spheroids was engineered. The system consists of two main parts: aggregation pillars and pick-and-place pillars. As the name implies, the former is used to aggregate spheroids and the latter is used to pick spheroids up once formed, and deposit them on culture surfaces according to a pre-determined pattern. The system is entirely 3D printed from biocompatible resin and can be used for cell culture purposes after minimal post-processing steps. Moreover, the system is compatible with commercial 24-well plates, making it easy to adopt in most labs. By modulating system dimensions, the size and shape of produced spheroids can be altered. As a proof of concept, the system was used to aggregate HT29 and MCF-7 cell lines, create different patterns, and create circular arrays of HT29 spheroids. The outcomes of this work contribute towards streamlining the process of spheroid generation and basic handling. Future work will focus on design enhancements to improve spheroid pick-up efficiency, improvement of the alignment features to allow for better precision in spheroid deposition, testing for the aggregation of more cell types, as well as increase the throughput of aggregation and patterning.

References

- 1. Mohs, R. C. & Greig, N. H. Drug discovery and development: Role of basic biological research. *Alzheimers Dement. Transl. Res. Clin. Interv.* **3**, 651–657 (2017).
- 2. Kraljevic, S., Stambrook, P. J. & Pavelic, K. Accelerating drug discovery. *EMBO Rep.* **5**, 837–842 (2004).
- 3. Donowitz, M., Turner, J. R., Verkman, A. S. & Zachos, N. C. Current and potential future applications of human stem cell models in drug development. *J. Clin. Invest.* **130**, 3342–3344 (2020).
- 4. Velasco, V., Shariati, S. A. & Esfandyarpour, R. Microtechnology-based methods for organoid models. *Microsyst. Nanoeng.* **6**, 1–13 (2020).
- 5. Karathanasis, S. K. Regenerative Medicine: Transforming the Drug Discovery and Development Paradigm. *Cold Spring Harb. Perspect. Med.* **4**, (2014).
- 6. Jensen, C. & Teng, Y. Is It Time to Start Transitioning From 2D to 3D Cell Culture? *Front. Mol. Biosci.* **7**, (2020).
- 7. Hsu, S.-H. & Hsieh, P.-S. Self-assembled adult adipose-derived stem cell spheroids combined with biomaterials promote wound healing in a rat skin repair model. *Wound Repair Regen.*Off. Publ. Wound Heal. Soc. Eur. Tissue Repair Soc. 23, 57–64 (2015).
- 8. Kawaguchi, S. *et al.* Intramyocardial Transplantation of Human iPS Cell–Derived Cardiac Spheroids Improves Cardiac Function in Heart Failure Animals. *JACC Basic Transl. Sci.* **6**, 239–254 (2021).

- 9. Wu, Y. C. *et al.* Transplantation of 3D adipose-derived stem cell/hepatocyte spheroids alleviates chronic hepatic damage in a rat model of thioacetamide-induced liver cirrhosis. *Sci. Rep.* **12**, 1227 (2022).
- 10. Gunti, S., Hoke, A. T. K., Vu, K. P. & London, N. R. Organoid and Spheroid Tumor Models: Techniques and Applications. *Cancers* **13**, 874 (2021).
- 11. Kim, J., Koo, B.-K. & Knoblich, J. A. Human organoids: model systems for human biology and medicine. *Nat. Rev. Mol. Cell Biol.* **21**, 571–584 (2020).
- 12. Andrews, M. G. & Kriegstein, A. R. Challenges of Organoid Research. *Annu. Rev. Neurosci.*45, 23–39 (2022).
- 13. Pinto, B., Henriques, A. C., Silva, P. M. A. & Bousbaa, H. Three-Dimensional Spheroids as In Vitro Preclinical Models for Cancer Research. *Pharmaceutics* **12**, 1186 (2020).
- 14. Nath, S. & Devi, G. R. Three-Dimensional Culture Systems in Cancer Research: Focus on Tumor Spheroid Model. *Pharmacol. Ther.* **163**, 94–108 (2016).
- 15. Langhans, S. A. Three-Dimensional in Vitro Cell Culture Models in Drug Discovery and Drug Repositioning. *Front. Pharmacol.* **9**, 6 (2018).
- 16. Gao, B., Jing, C., Ng, K., Pingguan-Murphy, B. & Yang, Q. Fabrication of three-dimensional islet models by the geometry-controlled hanging-drop method. *Acta Mech. Sin.* **35**, 329–337 (2019).
- Raghavan, S. et al. Comparative analysis of tumor spheroid generation techniques for differential in vitro drug toxicity. Oncotarget 7, 16948–16961 (2016).
- 18. Han, S. J., Kwon, S. & Kim, K. S. Challenges of applying multicellular tumor spheroids in preclinical phase. *Cancer Cell Int.* **21**, 152 (2021).

- 19. Metzger, W. *et al.* The liquid overlay technique is the key to formation of co-culture spheroids consisting of primary osteoblasts, fibroblasts and endothelial cells. *Cytotherapy* **13**, 1000–1012 (2011).
- 20. Chan, B. P. & Leong, K. W. Scaffolding in tissue engineering: general approaches and tissue-specific considerations. *Eur. Spine J.* **17**, 467–479 (2008).
- 21. de la Zerda, A., Kratochvil, M. J., Suhar, N. A. & Heilshorn, S. C. Review: Bioengineering strategies to probe T cell mechanobiology. *APL Bioeng.* **2**, 021501 (2018).
- 22. Whitesides, G. M. The origins and the future of microfluidics. *Nature* **442**, 368–373 (2006).
- Olanrewaju, A., Beaugrand, M., Yafia, M. & Juncker, D. Capillary microfluidics in microchannels: from microfluidic networks to capillaric circuits. *Lab. Chip* 18, 2323–2347 (2018).
- 24. Beebe, D. J., Mensing, G. A. & Walker, G. M. Physics and Applications of Microfluidics in Biology. *Annu. Rev. Biomed. Eng.* **4**, 261–286 (2002).
- 25. Tung, Y.-C. *et al.* High-throughput 3D spheroid culture and drug testing using a 384 hanging drop array. *The Analyst* **136**, 473–478 (2011).
- 26. Zhao, L. *et al.* A 3D Printed Hanging Drop Dripper for Tumor Spheroids Analysis Without Recovery. *Sci. Rep.* **9**, 19717 (2019).
- 27. Frey, O., Misun, P. M., Fluri, D. A., Hengstler, J. G. & Hierlemann, A. Reconfigurable microfluidic hanging drop network for multi-tissue interaction and analysis. *Nat. Commun.* 5, 4250 (2014).

- 28. de Groot, T. E., Veserat, K. S., Berthier, E., Beebe, D. J. & Theberge, A. B. Surface-tension driven open microfluidic platform for hanging droplet culture. *Lab. Chip* **16**, 334–344 (2016).
- 29. Huang, S.-W., Tzeng, S.-C., Chen, J.-K., Sun, J.-S. & Lin, F.-H. A Dynamic Hanging-Drop System for Mesenchymal Stem Cell Culture. *Int. J. Mol. Sci.* **21**, 4298 (2020).
- 30. Cho, C.-Y. *et al.* Development of a Novel Hanging Drop Platform for Engineering Controllable 3D Microenvironments. *Front. Cell Dev. Biol.* **8**, (2020).
- 31. Kim, H., Roh, H., Kim, H. & Park, J.-K. Droplet contact-based spheroid transfer technique as a multi-step assay tool for spheroid arrays. *Lab. Chip* **21**, 4155–4165 (2021).
- 32. Wales, D. J., Keshavarz, M., Howe, C. & Yeatman, E. 3D Printability Assessment of Poly(octamethylene maleate (anhydride) citrate) and Poly(ethylene glycol) Diacrylate Copolymers for Biomedical Applications. *ACS Appl. Polym. Mater.* **4**, 5457–5470 (2022).
- 33. Vieira, M. G. A., da Silva, M. A., dos Santos, L. O. & Beppu, M. M. Natural-based plasticizers and biopolymer films: A review. *Eur. Polym. J.* **47**, 254–263 (2011).
- 34. Gong, H., Bickham, B. P., Woolley, A. T. & Nordin, G. P. Custom 3D printer and resin for 18 μ m × 20 μ m microfluidic flow channels. *Lab. Chip* **17**, 2899–2909 (2017).
- 35. Urrios, A. *et al.* 3D-printing of transparent bio-microfluidic devices in PEG-DA. *Lab. Chip* **16**, 2287–2294 (2016).
- 36. Leung, B. M., Lesher-Perez, S. C., Matsuoka, T., Moraes, C. & Takayama, S. Media additives to promote spheroid circularity and compactness in hanging drop platform. *Biomater. Sci.* **3**, 336–344 (2015).

- 37. Kang, S.-M., Lee, J.-H., Huh, Y. S. & Takayama, S. Alginate Microencapsulation for Three-dimensional in vitro Cell Culture. *ACS Biomater. Sci. Eng.* **7**, 2864–2879 (2021).
- 38. Kojima, N., Tao, F., Mihara, H. & Aoki, S. Chapter 8 Methods for Engineering of Multicellular Spheroids to Reconstitute the Liver Tissue. in *Stem Cells and Cancer in Hepatology* (ed. Zheng, Y.-W.) 145–158 (Academic Press, 2018). doi:10.1016/B978-0-12-812301-0.00008-6.